SMAI-JCM
SMAI Journal of Computational Mathematics

Design and analysis of a Schwarz coupling method for 3D Navier–Stokes equations and 2D Shallow Water equations

Manel Tayachi, Céline Acary-Robert & Éric Blayo

Volume 12 (2026), p. 1-26.
https://doi.org/10.5802/jcm.141

The SMAI Journal of Computational Mathematics is a member of the Centre Mersenne for Open Scientific Publishing
http://www.centre-mersenne.org/
Submissions at https://smai-jcm.centre-mersenne.org/ojs/submission
e-ISSN: 2426-8399

SMAI Journal of Computational Mathematics
Vol. 12, 1-26 (2026)

Design and analysis of a Schwarz coupling method for 3D Navier–Stokes equations and 2D Shallow Water equations

Manel Tayachi [1]
Céline Acary-Robert [2]
Éric Blayo [3]

[1] Université Grenoble Alpes, CNRS, Grenoble INP, LJK, Grenoble, France
E-mail address: manel.tayachi@univ-grenoble-alpes.fr
[2] Université Grenoble Alpes, Inria, CNRS, Grenoble INP, LJK, Grenoble, France
E-mail address: celine.acary-robert@univ-grenoble-alpes.fr
[3] Université Grenoble Alpes, Inria, CNRS, Grenoble INP, LJK, Grenoble, France
E-mail address: eric.blayo@univ-grenoble-alpes.fr.

Abstract. We propose in the present work an iterative coupling method for a dimensionally heteregeneous problem. We consider the 3D linearized hydrostatic Navier–Stokes equations coupled with corresponding 2D linearized shallow water equations. We first show briefly how to derive the 2D linearized shallow water system from the 3D linearized hydrostatic Navier–Stokes system. Then we propose and study a Schwarz-like algorithm to couple the two systems and we prove under some assumptions that the convergence of this Schwarz algorithm is equivalent to the convergence of the classical domain decomposition algorithm of shallow water equations. Finally, we give some theoretical results related to the control of the difference between a global 3D reference solution and the 3D part of the coupled solution. These results are illustrated numerically.

2020 Mathematics Subject Classification. 65M55.

Keywords. dimensionally heterogeneous coupling; domain decomposition; multiscale analysis; hydrostatic Navier–Stokes equations, shallow water equations.

1. Introduction

Modeling complex phenomena, such as some hydrodynamical ones, may require the use of several mathematical and numerical models rather than using a single system of equations. One can for example replace locally the most general (often complex) model, such as the 3D Navier–Stokes system, with simpler models when physics allows it. The simpler models could in particular work in lower dimensions than the dimension of the most general model. For example, the 2D shallow water equations can locally replace the 3D Navier–Stokes system, as they are derived from this set of equations by vertical integration under the assumption of a small domain aspect ratio. One has thus to deal with a dimensionally heterogeneous coupling problem. Such a coupling between a mD model and a nD model where $n > m$ may limit the need for heavy computations and lead to efficient results. In the context of hydrodynamics, such coupled problems were studied in many works and used in several situations. For example, to model blood flows in compliant vessels, Formaggia et al. proposed in [10] to couple the 1D and the 3D Navier–Stokes equations. Miglio et al. [22], Marin and Monnier [20], Finaud-Guyot et al. [9] and Malleron et al. [19] have coupled the 1D and 2D shallow water equations in the context of river flows. Leiva et al. [17] also used dimensionally heteregeneous models in the context of fluid mechanics. In [29], we investigated such a dimensionally heterogeneous coupling problem on the academic case of a 2D Laplace equation with non-symmetric boundary conditions coupled with a corresponding 1D Laplace equation obtained by vertical integration of the 2D equation. To tackle this problem,

https://doi.org/10.5802/jcm.141

we proposed and analysed an efficient Schwarz-like algorithm (Schwarz methods will be described in Section 3). Similar test cases were addressed by Blanco et al. in [4] and by Panasenko [24] but with different coupling methodologies (variational approach in [4] and asymptotic partial decomposition of domain in [24]). The main difference between the approaches presented in [4] and [24] and those of [29] is the choice of the coupling method. Note that other types of complex coupled problems arise in other contexts, which are out of the scope of the present paper, like multiscale modeling (e.g. micro-macro approaches in [15]) or coupling between a continuous model and a discrete model (e.g. for rarefied gases in [25]).

In [29] the use of a Schwarz-like method was motivated by the need of a non-intrusive computational approach. Indeed the Schwarz algorithms, developed initially in the context of domain decomposition, do not require changes in the models, but only some exchange of information through boundary conditions. Different strategies can thus be used for space discretization in each subdomain. Besides, the choice of different time steps is also possible, by using the so-called Schwarz *global-in-time* or *waveform relaxation* algorithms [11, 12, 13]. However, due to their iterative nature, these Schwarz algorithms may generate huge computations. It is therefore useful to optimize the interface conditions in order to accelerate the convergence. From a theoretical point of view, the so-called *perfectly transparent* or *perfectly absorbing* boundary conditions allow an exact convergence in only two iterations. Nevertheless, they are generally non-local in space and/or time, which represents a major obstacle to their direct use, and leads to the quest for local approximations. The situation is even further complicated for dimensionally heterogeneous coupled problems by the addition of extension and restriction operators.

In the context of river flow modeling, one can consider 2D (or even 1D) shallow water equations in many parts of rivers, and 3D Navier–Stokes equations where 3D effects cannot be neglected. Numerical experiments were already performed for such configurations, e.g. in [7] and [23], with efficient performances. Nevertheless, theoretical analysis is still lacking. As an intermediate step in this direction, and in the continuity of [6] and [29], the objective of the present work is to design and analyse such an algorithm for the corresponding linearized systems. We prove that under some assumptions the convergence of the coupling algorithm is equivalent to the convergence of the Schwarz waveform relaxation algorithm for linear viscous shallow water equations designed and studied in [6]. Furthermore we provide a control bound of the modeling error due the reduction of dimension as a function of the coupling interfaces positions.

This paper is organized as follows: in Section 2 we introduce the 3D linearized hydrostatic Navier–Stokes equations and we briefly show how to derive the 2D linearized shallow water equations. We then define the coupling problem. In Section 3 we define the Schwarz waveform relaxation algorithm and we prove that the convergence of this algorithm is equivalent to the convergence of the classic domain decomposition algorithm for the shallow water system if the bottom friction is neglected. Then we briefly study the well-posedness of the algorithm with Robin-like interface conditions. In Section 4, we prove a theoretical result related to the control of the difference between the 3D part of the coupled solution and the global 3D solution. Finally, Section 5 presents numerical illustrations of the convergence of the classic domain decomposition method for the linearized shallow water system with viscosity, and of the convergence of the coupling algorithm. It also illustrates the influence of the interface position on the coupled solution.

2. **Coupled models**

In order to derive an efficient coupling algorithm between the 3D hydrostatic Navier–Stokes equations and the 2D shallow water system, we first write the linearized approximation of the 3D hydrostatic Navier–Stokes equations and derive the corresponding 2D linearized shallow water system.

2.1. **Hydrostatic Navier–Stokes equations**

We consider the hydrostatic Navier–Stokes equations:

$$\begin{cases} \partial_t \mathbf{U}_h + \mathbf{U}.\nabla_h \mathbf{U}_h - \mu \Delta \mathbf{U}_h + \dfrac{1}{\rho}\nabla_h p = 0 \\ \qquad\qquad \operatorname{div}_h \mathbf{U}_h + \partial_z W = 0 \\ \qquad\qquad\qquad\qquad \partial_z p = -\rho g \end{cases} \tag{2.1}$$

in the domain $(x, y, z, t) \in \Omega_t \times (0, T) = \omega \times [-H, \zeta(x, y, t)] \times (0, T)$, where ω is an open domain of $\mathbb{R}^2$, T denotes the length of the considered time period ($0 < T < +\infty$), $\zeta(x, y, t)$ denotes the free surface height, and the depth H is constant (flat bottom). The unknowns are the velocity $\mathbf{U} = (\mathbf{U}_h, W) = (U, V, W)$ and the pressure p. The density ρ and the kinematic viscosity μ are assumed constant.

This set of equations is derived from the incompressible Navier–Stokes equations by introducing the small aspect ratio $\varepsilon = \frac{H}{L}$, where L is the horizontal characteristic length, and considering the hydrostatic approximation which consists in fixing $\varepsilon = 0$ in the equation for W in the nondimensional system [18].

These equations are supplemented with initial and boundary conditions. At the bottom of the domain ($\Gamma_B = \{z = -H\}$), we impose a non-penetration condition and a frictionless condition:

$$W(x, y, -H, t) = 0 \tag{2.2}$$

and

$$\mu\, \partial_z \mathbf{U}_{h|z=-H} = 0 \tag{2.3}$$

At the free surface $\Gamma_T = \{z = \zeta(x, y, t)\}$, we impose a kinematic boundary condition and the balance of the stresses:

$$\partial_t \zeta + \mathbf{U}_{h|z=\zeta}.\nabla_h \zeta - W_{|z=\zeta} = 0 \tag{2.4}$$

and

$$\boldsymbol{\sigma}.\mathbf{n} = 0 \tag{2.5}$$

where $\mathbf{n}$ is the outward normal vector to the free surface and $\boldsymbol{\sigma} = -pI + \mu(\nabla \mathbf{U} + \nabla \mathbf{U}^t)$ is the constraint tensor. We neglect here the atmospheric pressure.

At the lateral boundaries, we impose Dirichlet boundary conditions:

$$\mathbf{U}_h = \mathbf{U}^d \quad \text{on } \partial\Omega_t \setminus (\Gamma_B \cup \Gamma_T) \times (0, T) \quad \text{and} \quad \zeta = \zeta^d \quad \text{on } \partial\omega \times (0, T)$$

and in the case of an unbounded domain ω, we impose homogeneous Dirichlet boundary conditions when $\|(x, y)\| \to \infty$.

Finally, initial conditions are provided:

$$\mathbf{U}_h(\,\cdot\,, 0) = \mathbf{U}_h^{ini} \quad \text{in } \Omega_0 \quad \text{and} \quad \zeta(\,\cdot\,, 0) = \zeta^{ini} \quad \text{in } \omega$$

Remark 2.1. In the case of the ocean, the set of hydrostatic equations is supplemented with equations for temperature, salinity and density, and a Coriolis term is also added, leading to the so-called "primitive equations" (e.g. [18]).

2.2. **Linearized hydrostatic Navier–Stokes equations**

The hydrostatic Navier–Stokes system can be transformed into an equivalent form, as in [3] or in [8]. Using the continuity equation and the non-penetration condition, the vertical velocity W can be written as a function of the horizontal velocity $\mathbf{U}_h$ and, as shown in [8], one can prove by using the Leibniz rule that the kinematic condition (2.4) is equivalent to a free surface equation. One can then

write the pressure p as a function of the free surface ζ using the hydrostatic condition, and the set of equations becomes:

$$\begin{cases} \partial_t \mathbf{U}_h + \mathbf{U}.\nabla \mathbf{U}_h - \mu \Delta \mathbf{U}_h + g \nabla_h \zeta = 0 & \text{in } \Omega_t \times (0,T) \\ \operatorname{div}_h \mathbf{U}_h + \partial_z W = 0 & \text{in } \Omega_t \times (0,T) \\ \partial_t \zeta + \operatorname{div}_h \left(\displaystyle\int_{-H}^{\zeta} \mathbf{U}_h \, \mathrm{d}z \right) = 0 & \text{in } \omega \times (0,T) \end{cases} \tag{2.6}$$

In order to set up a Schwarz algorithm and to prove its convergence, we now linearize the problem around a constant velocity $(\mathbf{U}_0, w_0) = (u_0, v_0, 0)$ and the reference value $\zeta_0 = 0$ of the free surface. Such a linearization is a usual tool to get theoretical results for non linear equations. Such results are helpful for actual applications since the reference state used for the linearization can be updated all along the model trajectory. The linearized system reads (see [3] for more details):

$$\begin{cases} \partial_t \mathbf{U}_h^G + \mathbf{U}_0.\nabla_h \mathbf{U}_h^G - \mu \Delta \mathbf{U}_h^G + g \nabla_h \zeta = 0 & \text{in } \Omega \times (0,T) = \omega \times [-H,0] \times (0,T) \\ \partial_t \zeta + H \operatorname{div}_h(\overline{\mathbf{U}}_h^G) + \mathbf{U}_0.\nabla_h \zeta = 0 & \text{in } \omega \times (0,T) \\ \mu \, \partial_z \mathbf{U}_h^G = 0 & \text{at } z = 0 \\ \mu \partial_z \mathbf{U}_h^G = 0 & \text{at } z = -H \\ \mathbf{U}_h^G = \mathbf{U}^d & \text{on } \partial\Omega \setminus (\Gamma_B \cup \Gamma_T) \times (0,T) \\ \zeta = \zeta^d & \text{on } \partial\omega \times (0,T) \\ \mathbf{U}_h^G(\,\cdot\,,0) = \mathbf{U}_h^{ini} & \text{in } \Omega \\ \zeta(\,\cdot\,,0) = \zeta^{ini} & \text{in } \omega \end{cases} \tag{2.7}$$

where the superscript G refers to what we will call the *global reference solution*, i.e. the solution of the linearized hydrostatic Navier–Stokes equations throughout the whole domain Ω. The overbar denotes the averaging operator in the vertical direction, defined by:

$$\overline{f} = \frac{1}{H} \int_{-H}^{0} f(z) \, \mathrm{d}z$$

The vertical velocity W^G can be obtained from:

$$\begin{cases} \operatorname{div}_h \mathbf{U}_h^G + \partial_z W^G = 0 & \text{in } \Omega \times (0,T) \\ W^G(x,y,-H,t) = 0 \end{cases} \tag{2.8}$$

In the sequel, similarly to the approach taken in [29], we want to take advantage of the shallowness of Ω to derive a relevant simplified model that can locally replace the global model (2.7). We then introduce the following definition:

Definition 2.2. Let Ω_{2D} be the subset of Ω in which 3D effects may be neglected, and $\Omega_{3D} = \Omega \backslash \Omega_{2D}$ the subset of Ω in which 3D effects cannot be neglected.

Remark 2.3. As indicated in [29], the definition of Ω_{3D} depends of course on several features, such as the domain aspect ratio, the considered system of equations, forcing terms (including boundary conditions), initial condition, etc.

We also assume that there exists L_1 such that $\Omega_{2D} = \Omega \cap \{x < L_1\}$ and $\Omega_{3D} = \Omega \cap \{x > L_1\}$. Thus, the interface Γ between the two subdomains Ω_{2D} and Ω_{3D} is located at $x = L_1$. For the sake of simplicity, we suppose that L_1 is independent of time. We will now replace the 3D linearized hydrostatic Navier–Stokes equations in Ω_{2D} by 2D linearized shallow water equations, and study the resulting coupled 2D/3D problem (see Figure 2.1).

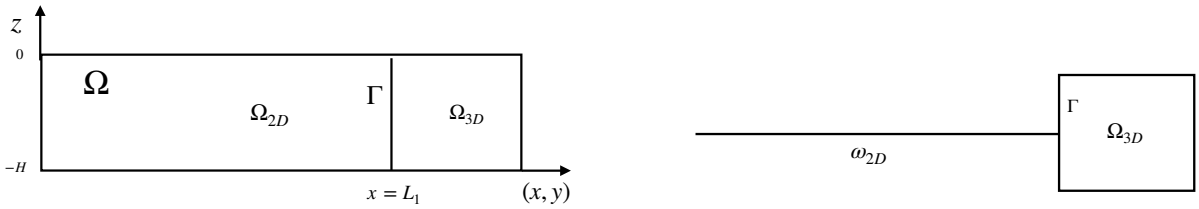

FIGURE 2.1. Left panel: 3D reference domain Ω. Right panel: coupled configuration, where the right part of Ω ($x < L_1$) is replaced by the subdomain Ω_{2D}, where simplified 2D shallow water equations will be solved instead of the 3D equations.

2.3. **Linearized Shallow Water equations**

The linearized shallow water system is obtained by averaging system (2.7). Due to the frictionless condition at the bottom, we do not need to make any other approximation as in [14]. With U a characteristic scale for the horizontal velocity and assuming now that the horizontal characteristic length L is equal to L_1, we can introduce the following dimensionless variables and numbers:

$$(x, y) = L_1(\widetilde{x}, \widetilde{y}), \quad z = H\widetilde{z}, \quad t = \frac{L_1}{U}\widetilde{t}, \quad \mathbf{U}_h = U\widetilde{\mathbf{U}}_h, \quad \zeta = H\widetilde{\zeta}$$

and

$$\nu = \frac{1}{Re} = \frac{\mu}{L_1 U}, \quad Fr = \frac{U}{\sqrt{gH}}$$

Therefore we have the following result:

Lemma 2.4. *The linearized shallow water system*

$$\begin{cases} \partial_t \zeta + H \operatorname{div}_h(\mathbf{u}) + \mathbf{U}_0.\nabla_h \zeta = 0 \\ \partial_t \mathbf{u} + (\mathbf{U}_0.\nabla_h)\mathbf{u} - \mu \Delta_h \mathbf{u} + g \nabla_h \zeta = 0 \end{cases} \tag{2.9}$$

results from an approximation in $O(\varepsilon^2)$ of the linearized hydrostatic Navier–Stokes equations in Ω_{2D} where $\varepsilon = \frac{H}{L_1}$. Moreover:

$$\mathbf{U}_h^G(x, y, z, t) = \mathbf{u}(x, y, t) + O(\varepsilon^2) \quad \textit{for all} \quad (x, y, z, t) \in \Omega_{2D} \times (0, T) \tag{2.10}$$

Proof. The proof being quite similar to the one given in [14], we only give here the outline and refer to [14] for more details. First, by rescaling the system (2.7), we obtain (we omit the $\widetilde{\ }$ for the sake of clarity):

$$\begin{cases} \partial_t \mathbf{U}_h^G + \mathbf{U}_0.\nabla_h \mathbf{U}_h^G - \nu \Delta_h \mathbf{U}_h^G - \dfrac{\nu}{\varepsilon^2}\partial_z^2 \mathbf{U}_h^G + \dfrac{1}{Fr^2}\nabla_h \zeta = 0 & \text{in } \omega_{2D} \times [-1, 0] \times (0, T) \\ \partial_t \zeta + \operatorname{div}_h(\overline{\mathbf{U}}_h) + \mathbf{U}_0.\nabla_h \zeta = 0 & \text{in } \omega_{2D} \times (0, T) \\ \nu \partial_z \mathbf{U}_h^G = 0 & \text{at } z = 0 \\ \nu \partial_z \mathbf{U}_h^G = 0 & \text{at } z = -1 \\ \mathbf{U}_h^G(\,\cdot\,, 0) = \mathbf{U}^{ini} & \text{in } \omega_{2D} \times [-1, 0] \\ \zeta(\,\cdot\,, 0) = \zeta^{ini} & \text{in } \omega_{2D} \end{cases} \tag{2.11}$$

Let suppose as in [14] that $\nu = \varepsilon \nu_0$. Thus, we deduce from the momentum equation and from the boundary condition at the bottom that $\partial_z \mathbf{U}_h^G = O(\varepsilon)$. Then integrating between -1 and z, the

following first order relation holds:

$$\mathbf{U}_h^G(x,y,z,t) = \mathbf{U}_h^G(x,y,-1,t) + O(\varepsilon) \tag{2.12}$$

$$= \overline{\mathbf{U}}_h^G(x,y,t) + O(\varepsilon) \tag{2.13}$$

Now, averaging the momentum equation in (2.11) between -1 and 0 yields:

$$\partial_t \overline{\mathbf{U}}_h^G + (\mathbf{U}_0.\nabla_h)\overline{\mathbf{U}}_h^G + \frac{1}{Fr^2}\nabla_h\zeta = \nu\Delta_h\overline{\mathbf{U}}_h^G \tag{2.14}$$

By keeping just the first order terms on ε in (2.14), we obtain:

$$\partial_t \overline{\mathbf{U}}_h^G + (\mathbf{U}_0.\nabla_h)\overline{\mathbf{U}}_h^G + \frac{1}{Fr^2}\nabla_h\zeta = O(\varepsilon) \tag{2.15}$$

The first equations of (2.11), (2.12) and (2.15) give:

$$\begin{aligned}\frac{\nu_0}{\varepsilon}\partial_z^2\mathbf{U}_h^G &= \partial_t\mathbf{U}_h^G + \mathbf{U}_0.\nabla\mathbf{U}_h^G - \nu\Delta_h\mathbf{U}_h^G + \frac{1}{Fr^2}\nabla_h\zeta \\ &= \partial_t\overline{\mathbf{U}}_h^G + \mathbf{U}_0.\nabla\overline{\mathbf{U}}_h^G + \frac{1}{Fr^2}\nabla_h\zeta + O(\varepsilon) \\ &= O(\varepsilon)\end{aligned}$$

By integrating between z and 0 we obtain:

$$\partial_z\mathbf{U}_h^G = O(\varepsilon^2)$$

Then, by integrating this time between -1 and z, we have:

$$\mathbf{U}_h^G = \mathbf{U}_h^G|_{z=-1} + O(\varepsilon^2) \tag{2.16}$$

Thus we deduce the second order relation:

$$\overline{\mathbf{U}}_h^G = \mathbf{U}_h^G|_{z=-1} + O(\varepsilon^2) \tag{2.17}$$

Hence the final result, after a back transformation into dimensional variables. ∎

Remark 2.5. If we consider an additional bottom friction term, the boundary condition (2.3) becomes:

$$-\mu\,\partial_z\mathbf{U} + \kappa\mathbf{U}_h = 0 \quad \text{at } z = -H \tag{2.18}$$

By introducing the dimensionless variable $K = \frac{\kappa}{U} = K_0\varepsilon$ and assuming as in [14] that $K_0 = 0(1)$ (a small friction) then the term $\frac{\kappa}{1+\frac{\kappa H}{3\mu}}\,\mathbf{u}$ must be added into the left-hand side of the second equation of system (2.9).

Moreover, the second order relation (2.10) becomes $\mathbf{U}_h^G(x,y,z,t) = \mathbf{u}(x,y,t)(\alpha+\beta(z^2-H^2))+O(\varepsilon^2)$ where α and β are constants. More details about how to derive the shallow water equations when a small friction is considered on the bottom can be found in [14]. Now, if we suppose that $K_0 = O(\varepsilon)$, then we still have the shallow water system (2.9) and the second order relation (2.10).

2.4. **The coupling problem**

Once a criterion has been defined to quantify 3D effects, we have seen that Ω_{2D} and Ω_{3D} are supposed to be separated by an interface $x = L_1$. However, in practice, we do not know its exact location. On the other hand, we generally know a value L_2 such that we are sure that the 3D effects are significant for $x > L_2$. So, in practice, we will choose a value $L_0 < L_2$ and place our interface at $x = L_0$ (but with no full guarantee that L_0 will indeed be smaller than the optimal value L_1).

For the sake of simplicity we suppose here that $L_0 = 0$. Thus we consider the linearized shallow water system in $\Omega^- = \omega^- \times [-H, 0]$, where $\omega^- = \omega \cap \{x < 0\}$, and we keep the 3D linearized hydrostatic Navier–Stokes equations in $\Omega^+ = \omega^+ \times [-H, 0]$, where $\omega^+ = \omega \cap \{x > 0\}$. We denote by Γ the common

2D interface between these two non-overlapping subdomains Ω^- and Ω^+: $\Gamma = \{x = 0\}$. We also denote by γ the 1D interface between ω^- and ω^+.

We then consider the two following systems:

$$\begin{cases} \partial_t \mathbf{u} + (\mathbf{U}_0.\nabla_h)\mathbf{u} + g\nabla_h\zeta - \mu\Delta_h\mathbf{u} = 0 & \text{in } \omega^- \times (0,T) & (2.19a) \\ \partial_t\zeta + H\ \mathrm{div}_h(\mathbf{u}) + \mathbf{U}_0.\nabla_h\zeta_- = 0 & \text{in } \omega^- \times (0,T) & (2.19b) \\ (\mathbf{u},\zeta_-) = \left(\overline{\mathbf{U}}_-^d, \zeta_-^d\right) & \text{on } \partial\omega_{out}^- \times (0,T) & (2.19c) \\ \mathbf{u}(\,\cdot\,,0) = \overline{\mathbf{U}}_-^{ini} & \text{in } \omega^- & \\ \text{and} \quad \zeta_-(\,\cdot\,,0) = \zeta_-^{ini} & \text{in } \omega^- & (2.19d) \end{cases}$$

and

$$\begin{cases} \partial_t \mathbf{U}_h + (\mathbf{U}_0.\nabla_h)\mathbf{U}_h - \mu\Delta\mathbf{U}_h + g\nabla_h\zeta_+ = 0 & \text{in } \Omega^+ \times (0,T) & (2.20a) \\ \partial_t\zeta_+ + H\ \mathrm{div}_h(\overline{\mathbf{U}}_h) + \mathbf{U}_0.\nabla_h\zeta_+ = 0 & \text{in } \omega^+ \times (0,T) & (2.20b) \\ \mu\partial_z\mathbf{U}_h = 0 & \text{at } z = 0 & (2.20c) \\ \mu\partial_z\mathbf{U}_h = 0 & \text{at } z = -H & (2.20d) \\ \mathbf{U}_h = \mathbf{U}_+^d & \text{in } (\partial\Omega_{out}^+ \setminus \Gamma_B \cup \Gamma_T) \times (0,T) & (2.20e) \\ \zeta_+ = \zeta_+^d & \text{in } \partial\omega_{out}^+ \times (0,T) & (2.20f) \\ \mathbf{U}_h(\,\cdot\,,0) = \mathbf{U}_+^{ini} & \text{in } \Omega^+ & \\ \text{and} \quad \zeta_+(\,\cdot\,,0) = \zeta_+^{ini} & \text{in } \omega^+ & (2.20g) \end{cases}$$

where the boundaries $\partial\omega_{out}^-$ and $\partial\Omega_{out}^+$ are respectively $\partial\omega^- \setminus \gamma$ and $\partial\Omega^+ \setminus \Gamma$. These two systems are to be coupled through the interfaces γ and $\Gamma = \gamma \times [-H, 0]$ by defining interface conditions under the form:

$$\mathcal{B}_-(\mathbf{u},\zeta_-) = \mathcal{B}_-(\mathcal{R}(\mathbf{U}_h),\zeta_+) \quad \text{on } \gamma \times (0,T) \tag{2.21}$$

$$\mathcal{B}_+(\mathbf{U}_h,\zeta_+) = \mathcal{B}_+(\mathcal{E}(\mathbf{u}),\zeta_-) \quad \text{on } \Gamma \times (0,T) \tag{2.22}$$

Operators $\mathcal{R}$ and $\mathcal{E}$ are respectively a restriction (or projection) on γ and an extension on Γ to be defined, and the boundary operators $\mathcal{B}_-$ and $\mathcal{B}_+$ are to be determined.

In order to set up an efficient Schwarz coupling algorithm in the next section, we first need to define the coupling notion by itself, that is, defining the quantities or values to be exchanged between the two models through the coupling interfaces. Let us first define the natural transmission conditions of system (2.7):

Lemma 2.6. *The natural transmission condition of system* (2.7) *through the interface* Γ*, obtained by a simple variational formulation, is the continuity of:*

$$\left(\mu\partial_x\mathbf{U}_h^G - u_0\mathbf{U}_h^G - g\begin{pmatrix}\zeta\\0\end{pmatrix}, u_0\zeta + H\overline{U}_h^G\right) \tag{2.23}$$

Proof. The proof is quite similar to the one given in [6], so we refer to this work for more details. ■

As a consequence in our case, a natural formulation of the coupled problem is the following:

Definition 2.7. The coupled problem is defined by systems (2.19) and (2.20), with the following interface conditions on γ:

$$\mu\partial_x \mathbf{u} - u_0\mathbf{u} - g\begin{pmatrix}\zeta_- \\ 0\end{pmatrix} = \mu\partial_x \overline{\mathbf{U}}_h - u_0\overline{\mathbf{U}}_h - g\begin{pmatrix}\zeta_+ \\ 0\end{pmatrix} \tag{2.24}$$

$$u_0\zeta_- + H\,u = u_0\zeta_+ + H\,\overline{U}_h \tag{2.25}$$

3. Schwarz multidimensional coupling algorithm

Several approaches can be used to couple different models: variational, algebraic or domain decomposition methods. We choose here a Schwarz domain decomposition approach, which has several practical advantages (simplicity for set-up, few changes in the numerical codes), see e.g. [12] for a general introduction to these methods. The Schwarz domain decomposition methods have been generalized to the case of heterogeneous spatial dimension coupling in [29].

3.1. Schwarz coupling algorithm

After having defined the coupling notion, we now set up a Schwarz coupling algorithm and solve it. We propose the following algorithm:

Algorithm 1. Schwarz multidimensional algorithm

Initialization : for $\mathbf{U}_h^0$ and ζ_+^0 given

At each iteration k ($k \geq 0$), solve :

$$\begin{cases} \mathcal{L}_{LSW}\Big(\mathbf{u}^{k+1}, \zeta_-^{k+1}\Big) = 0 & \text{in } (\omega^- \times (0,T))^2 \\ \mathcal{B}_-^{out}\Big(\mathbf{u}^{k+1}, \zeta_-^{k+1}\Big) = \overline{G}_-^{out} & \text{on } (\partial\omega_{out}^- \times (0,T))^2 \\ \mathcal{B}_-\Big(\mathbf{u}^{k+1}, \zeta_-^{k+1}\Big) = \mathcal{B}_-\Big(\mathcal{R}(\mathbf{U}_h^k), \zeta_+^k\Big) & \text{on } (\gamma \times (0,T))^2 \\ \mathbf{u}^{k+1}(\cdot\,,0) = \overline{\mathbf{U}}_-^{ini} & \text{in } \omega^- \\ \zeta_-^{k+1}(\cdot\,,0) = \zeta_-^{ini} & \text{in } \omega^- \end{cases}$$

then solve:

$$\begin{cases} \mathcal{L}_{LHNS}\Big(\mathbf{U}_h^{k+1}, \zeta_+^{k+1}\Big) = 0 & \text{in } \big(\Omega^+ \times (0,T)\big) \times \big(\omega^+ \times (0,T)\big) \\ \mathcal{B}_+^{out}\Big(\mathbf{U}_h^{k+1}, \zeta_+^{k+1}\Big) = G_+^{out} & \text{on } \big(\partial\Omega_{out}^+ \times (0,T)\big) \times \big(\partial\omega_{out}^+ \times (0,T)\big) \\ \mathcal{B}_+\Big(\mathbf{U}_h^{k+1}, \zeta_+^{k+1}\Big) = \mathcal{B}_+\Big(\mathcal{E}(\mathbf{u}^{k+1}), \zeta_-^{k+1}\Big) & \text{on } \big(\Gamma \times (0,T)\big) \times \big(\gamma \times (0,T)\big) \\ \mathbf{U}_h^{k+1}(\cdot\,,0) = \mathbf{U}_+^{ini} & \text{in } \Omega^+ \\ \zeta_+^{k+1}(\cdot\,,0) = \zeta_+^{ini} & \text{in } \omega^+ \end{cases}$$

The operator $\mathcal{L}_{LSW}$ denotes the set of equations (2.19a) and (2.19b) and the operator $\mathcal{L}_{LHNS}$ denotes the set of equations (2.20a) and (2.20b). The exterior boundaries are $\partial\omega_{out}^- = \partial\omega^- \setminus \gamma$, $\partial\Omega_{out}^+ = \partial\Omega^+ \setminus \Gamma$ and the operators $\mathcal{B}_-^{out}$ et $\mathcal{B}_+^{out}$ denote the exterior boundary conditions. The operators $\overline{G}_-^{out}$ and G_+^{out} take the values 0 or $(\overline{\mathbf{U}}_-^d, \zeta_-^d)$ and $(\mathbf{U}_+^d, \zeta_+^d)$ depending on if we have Neumann or Dirichlet conditions.

The operators $\mathcal{B}_-$ and $\mathcal{B}_+$ will be determined such that the algorithm converges and the natural transmission conditions (2.24) and (2.25) are satisfied. Their choice is crucial in order to set up an efficient coupling algorithm with optimal convergence.

As in [4] and [29] we can define the restriction and extension operators $\mathcal{R}$ and $\mathcal{E}$ by:

$$\begin{aligned} \mathcal{R} : \Lambda_{3D} \times (0,T) &\longrightarrow \Lambda_{2D} \times (0,T) \qquad \text{and} \qquad \mathcal{E} : \Lambda_{2D} \times (0,T) \longrightarrow \Lambda_{3D} \times (0,T) \\ (\mathbf{U})|_{\Gamma\times(0,T)} &\longmapsto (\mathcal{R}\mathbf{U})|_{\gamma\times(0,T)} \qquad\qquad (\mathbf{u})|_{\gamma\times(0,T)} \longmapsto (\mathcal{E}\mathbf{u})|_{\Gamma\times(0,T)} \end{aligned}$$

where Λ_{2D} and Λ_{3D} denote the trace spaces on the interface γ for the 2D spatial functions and on Γ for the 3D spatial functions. In view of the derivation of the linearized shallow water system from linearized Navier–Stokes equations, we define the restriction operator $\mathcal{R}$ as the vertical average:

$$\begin{aligned} \mathcal{R} : \Lambda_{3D} \times (0,T) &\longrightarrow \Lambda_{2D} \times (0,T) \\ (\mathbf{U}_h)_{|\Gamma\times(0,T)} &\longmapsto \frac{1}{H}\int_{-H}^{0} (\mathbf{U}_h)_{|\Gamma\times(0,T)}\,\mathrm{d}z \end{aligned}$$

that is $\mathcal{R}(\mathbf{U}_h)(0,y,t) = \frac{1}{H}\int_{-H}^{0}\mathbf{U}_h(0,y,z,t)\,\mathrm{d}z$.

Now, in view of the second order relations (2.16) and (2.17), we may define the extension operator $\mathcal{E}$ by:

$$\begin{aligned} \mathcal{E} : \Lambda_{2D} \times (0,T) &\longrightarrow \Lambda_{3D} \times (0,T) \\ (\mathbf{u})|_{\gamma\times(0,T)} &\longmapsto (\mathbf{u})|_{\Gamma\times(0,T)} \end{aligned}$$

that is $\mathcal{E}(\mathbf{u})(0,y,z,t) = \mathbf{u}(0,y,t)$. In other words, as we assumed a frictionless condition at the bottom, the quantities coming from the 2D model are extended uniformly along the vertical axis through the interface Γ. Note that this could be no longer true if there is an additional bottom friction term. In fact, depending on the amplitude of the friction coefficient, the distribution through the interface could be parabolic, see [14].

Remark 3.1. Note that the time interval $(0,T)$, if long, can be divided into several successive time windows over each of which the algorithm is applied.

3.2. **Rewriting the Schwarz algorithm**

In this section we study the convergence of the Schwarz Algorithm 1. But in order to simplify the theoretical study of the coupling algorithm, we first rewrite it by decomposing the 3D velocity into vertical modes, which implies to find the spectrum of the operator $-\partial_z^2$ in $[-H,0]$ with homogeneous Neumann boundary conditions (see [5, 26, 27]).

Then we look for $\mathbf{U}_h$ under the form:

$$\mathbf{U}_h(x,y,z,t) = \sum_{n=0}^{\infty}\mathbf{U}_h^n(x,y,t)w_n(z) = \overline{\mathbf{U}}_h(x,y,t) + \sum_{n=1}^{\infty}\mathbf{U}_h^n(x,y,t)w_n(z)$$

where $w_n(z) = \alpha_n\cos(\frac{n\pi z}{H})$with $\alpha_0 = 1$ and $\alpha_n = \sqrt{2}\,(n>0)$ and $\overline{\mathbf{U}}_h(x,y,t) = \frac{1}{H}\int_{-H}^{0}\mathbf{U}_h(x,y,z,t)dz$ (the index n denotes here the rank of the vertical mode, not to be confused with Schwarz iteration index k). Note that, in the present case where the density is constant, the expansion corresponds to a simple Fourier series expansion, which ensures pointwise convergence or at least almost everywhere as soon as $\mathbf{U}_h$ is regular enough with respect to z.

By injecting this decomposition into (2.20), then multiplying by w_n and integrating between $-H$ and 0, we obtain (using the fact that $(w_n)_{n\geq 0}$ is an orthonormal basis):

- For $n = 0$, the first vertical mode (also called barotropic mode) $\mathbf{U}_h^0 = \overline{\mathbf{U}}_h$ coupled with the free surface is solution of the 2D linearized shallow water system in ω^+:

$$\begin{cases} \partial_t \overline{\mathbf{U}}_h + (\mathbf{U}_0.\nabla_h)\overline{\mathbf{U}}_h + g\nabla_h\zeta - \mu\Delta_h\overline{\mathbf{U}}_h = 0 & \text{in } \omega^+ \times (0,T) \\ \partial_t\zeta + H\ \mathrm{div}_h(\overline{\mathbf{U}}_h) + \mathbf{U}_0.\nabla_h\zeta = 0 & \text{in } \omega^+ \times (0,T) \\ \left(\overline{\mathbf{U}}_h, \zeta\right) = \left(\overline{\mathbf{U}}_+^d, \zeta_+^d\right) & \text{on } (\partial\omega_{out}^+ \times (0,T))^2 \\ \left(\overline{\mathbf{U}}_h(\,\cdot\,,0), \zeta(\,\cdot\,,0)\right) = \left(\overline{\mathbf{U}}_+^{ini}, \zeta_+^{ini}\right) & \text{in } (\omega^+)^2 \end{cases} \tag{3.1}$$

- For $n \geq 1$ (baroclinic modes) :

$$\partial_t \mathbf{U}_h^n + (\mathbf{U}_0.\nabla_h)\mathbf{U}_h^n - \mu\Delta_h\mathbf{U}_h^n + \frac{\mu(n\pi)^2}{H^2}\mathbf{U}_h^n = 0 \quad \text{in } \omega^+ \times (0,T) \tag{3.2}$$

The sum of the baroclinic modes $\mathbf{U}_b = \mathbf{U}_h - \overline{\mathbf{U}}_h$ is solution of the system:

$$\begin{cases} \dfrac{\partial \mathbf{U}_b}{\partial t} + (\mathbf{U}_0.\nabla_h)\mathbf{U}_b - \mu\Delta\mathbf{U}_b = 0 & \text{in } \Omega^+ \times (0,T) \\ \mathcal{B}_+^{out}(\mathbf{U}_b) = G_+^{out} - \overline{G}_+^{out} & \text{on } \partial\Omega_{out}^+ \times (0,T) \\ \mathbf{U}_b(\,\cdot\,,0) = \mathbf{U}_+^{ini} - \overline{\mathbf{U}}_+^{ini} & \text{in } \Omega^+ \end{cases} \tag{3.3}$$

We can then rewrite the Schwarz Algorithm 1 as follows:

Algorithm 2. Schwarz multidimensional coupling algorithm - Version 2

Initialization : $\mathbf{U}_h^0$ and ζ_+^0 given

At each iteration k ($k \geq 0$), solve:

$$\begin{cases} \mathcal{L}_{LSW}\left(\mathbf{u}^{k+1}, \zeta_-^{k+1}\right) = 0 & \text{in } (\omega^- \times (0,T))^2 \\ \mathcal{B}_-^{out}\left(\mathbf{u}^{k+1}, \zeta_-^{k+1}\right) = \overline{G}_-^{out} & \text{on } (\partial\omega_{out}^- \times (0,T))^2 \\ \mathcal{B}_-\left(\mathbf{u}^{k+1}, \zeta_-^{k+1}\right) = \mathcal{B}_-\left(\overline{\mathbf{U}}_h^k, \zeta_+^k\right) & \text{on } (\gamma \times (0,T))^2 \\ \mathbf{u}^{k+1}(\,\cdot\,,0) = \overline{\mathbf{U}}_-^{ini} & \text{in } \omega^- \\ \zeta_-^{k+1}(\,\cdot\,,0) = \zeta_-^{ini} & \text{in } \omega^- \end{cases}$$

then solve

$$\begin{cases} \mathcal{L}_{LSW}\left(\overline{\mathbf{U}}_h^{k+1}, \zeta_+^{k+1}\right) = 0 & \text{in } \left(\omega^+ \times (0,T)\right)^2 \\ \mathcal{B}_+^{out}\left(\overline{\mathbf{U}}_h^{k+1}, \zeta_+^{k+1}\right) = \overline{G}_+^{out} & \text{on } (\partial\omega_{out}^+ \times (0,T))^2 \\ \mathcal{B}_+^0\left(\overline{\mathbf{U}}_h^{k+1}, \zeta_+^{k+1}\right) = \mathcal{B}_+^0\left(\mathbf{u}^{k+1}, \zeta_-^{k+1}\right) & \text{on } (\gamma \times (0,T))^2 \\ \overline{\mathbf{U}}_h^{k+1}(\,\cdot\,,0) = \overline{\mathbf{U}}_+^{ini} & \text{in } \omega^+ \\ \zeta_+^{k+1}(\,\cdot\,,0) = \zeta_+^{ini} & \text{in } \omega^+ \end{cases}$$

and

$$\begin{cases} \mathcal{L}_{CD}\left((\mathbf{U}_b)^{k+1}\right) = 0 & \text{in } \Omega^+ \times (0,T) \\ \mathcal{B}_+^{out}\left((\mathbf{U}_b)^{k+1}\right) = G_+^{out} - \overline{G}_+^{out} & \text{on } \partial\Omega_{out}^+ \times (0,T) \\ \mathcal{B}'_+\left((\mathbf{U}_b)^{k+1}\right) = 0 & \text{on } \Gamma \times (0,T) \\ (\mathbf{U}_b)^{k+1}(\,\cdot\,,0) = \mathbf{U}_+^{ini} - \overline{\mathbf{U}}_+^{ini} & \text{in } \Omega^+ \end{cases}$$

where $\mathcal{B}_+^0$ denotes the restriction of the operator $\mathcal{B}_+$ for 2D spatial functions, $\mathcal{B}'_+$ is obtained from $\mathcal{B}_+$ by vanishing all terms containing ζ_+, and $\mathcal{L}_{CD}$ denotes the convection-diffusion operator $\partial_t + (\mathbf{U}_0.\nabla_h) - \mu\Delta$.

Due to this new form of the algorithm, we have then the following convergence result as a direct consequence of the Algorithm 2:

Lemma 3.2. *The coupling Algorithm 1 converges if and only if the classic domain decomposition algorithm of the linearized shallow water system defined by:* $\overline{\mathbf{U}}_h^0$ *and* ζ_+^0 *given*

$$\begin{cases} \mathcal{L}_{LSW}\left(\mathbf{u}_-^{k+1}, \zeta_-^{k+1}\right) = 0 & \text{in } (\omega^- \times (0,T))^2 \\ \mathcal{B}_-^{out}\left(\mathbf{u}_-^{k+1}, \zeta_-^{k+1}\right) = \overline{G}_-^{out} & \text{on } (\partial\omega_{out}^- \times (0,T))^2 \\ \mathcal{B}_-\left(\mathbf{u}_-^{k+1}, \zeta_-^{k+1}\right) = \mathcal{B}_-\left(\overline{\mathbf{U}}_h^k, \zeta_+^k\right) & \text{on } (\gamma \times (0,T))^2 \\ \left(\mathbf{u}_-^{k+1}, \zeta_-^{k+1}\right)(\cdot\,,0) = \left(\overline{\mathbf{U}}_-^{ini}, \zeta_-^{ini}\right) & \text{in } \omega^- \end{cases} \tag{3.4}$$

then

$$\begin{cases} \mathcal{L}_{LSW}\left(\overline{\mathbf{U}}_h^{k+1}, \zeta_+^{k+1}\right) = 0 & \text{in } (\omega^+ \times (0,T))^2 \\ \mathcal{B}_+^{out}\left(\overline{\mathbf{U}}_h^{k+1}, \zeta_+^{k+1}\right) = \overline{G}_+^{out} & \text{on } (\partial\omega_{out}^+ \times (0,T))^2 \\ \mathcal{B}_+^0\left(\overline{\mathbf{U}}_h^{k+1}, \zeta_+^{k+1}\right) = \mathcal{B}_+^0\left(\mathbf{u}_-^{k+1}, \zeta_-^{k+1}\right) & \text{on } (\gamma \times (0,T))^2 \\ \left(\overline{\mathbf{U}}_h^{k+1}, \zeta_+^{k+1}\right)(\cdot\,,0) = \left(\overline{\mathbf{U}}_+^{ini}, \zeta_+^{ini}\right) & \text{in } \omega^+ \end{cases} \tag{3.5}$$

converges, and the baroclinic velocity $\mathbf{U}_b = \mathbf{U}_h - \overline{\mathbf{U}}_h$ *is solution of the system:*

$$\begin{cases} \dfrac{\partial \mathbf{U}_b}{\partial t} + (\mathbf{U}_0.\nabla_h)\mathbf{U}_b - \mu\Delta\mathbf{U}_b = 0 & \text{in } \Omega^+ \times (0,T) \\ \mathcal{B}_+^{out}(\mathbf{U}_b) = G_+^{out} - \overline{G}_+^{out} & \text{in } \partial\Omega_{out}^+ \times (0,T) \\ \mathcal{B}'_+(\mathbf{U}_b) = 0 & \text{on } \Gamma \times (0,T) \\ \mathbf{U}_b(\cdot\,,0) = \mathbf{U}_+^{ini} - \overline{\mathbf{U}}_+^{ini} & \text{in } \Omega^+ \end{cases}$$

Remark 3.3. Note that this result is no longer true if there is an additional bottom friction term, since the vertical modes of the operator $-\partial_z^2$ cannot be decoupled in this case, see [3].

3.3. **Study of the coupling algorithm with "Robin boundary" conditions**

We investigated in [6] the convergence of the domain decomposition algorithm for the linearized shallow water system. We first studied the approximation of the optimal transmission conditions by assuming a large Reynolds number and a small ratio aspect ε, as in Section 2.3. Unfortunately we were not able to find a useful approximation of these operators. Therefore we studied the domain decomposition algorithm with "Robin" boundary conditions. More precisely we studied the convergence of the algorithm with the following boundary conditions (for $u_0 > 0$):

$$\mathcal{B}_-(\mathbf{u},\zeta) = \begin{pmatrix} \mu\dfrac{\partial u}{\partial x} - g\zeta + \dfrac{(\lambda - u_0)}{2}u \\ \mu\dfrac{\partial v}{\partial x} + \dfrac{(\lambda - u_0)}{2}v \end{pmatrix} \tag{3.6}$$

and

$$\mathcal{B}_+^0(\mathbf{u},\zeta) = \begin{pmatrix} -\mu\dfrac{\partial u}{\partial x} + g\zeta + \dfrac{(\lambda + u_0)}{2}u \\ -\mu\dfrac{\partial v}{\partial x} + \dfrac{(\lambda + u_0)}{2}v \\ u_0\zeta \end{pmatrix} \tag{3.7}$$

where λ is an artificially introduced positive constant whose value will be optimized to accelerate the convergence of the algorithm, while still guaranteeing that coupling conditions (2.24)-(2.25) will be satisfied by the converged coupled solution.

We can extend the operator $\mathcal{B}_+$ defined by (3.7) in the case of 3D spatial functions:

$$\mathcal{B}_+(\mathbf{U}_h,\zeta)=\begin{pmatrix} -\mu\dfrac{\partial U}{\partial x}+g\zeta+\dfrac{(\lambda+u_0)}{2}U \\ -\mu\dfrac{\partial V}{\partial x}+\dfrac{(\lambda+u_0)}{2}V \\ u_0\zeta \end{pmatrix} \tag{3.8}$$

and redefine the Schwarz Algorithm 2 with the operators (3.6) and (3.8).

Proposition 3.4. *The coupling algorithms 1 and 2 defined with the operators* (3.6), (3.7) *and* (3.8) *are well-posed. The sequences* $(\mathbf{u}^{k+1},\zeta_-^{k+1})$ *and* $(\mathbf{U}_h^{k+1},\zeta_+^{k+1})$ *defined by the algorithms 1 and 2 converge to* $(\mathbf{u}|_{\omega^-},\zeta|_{\omega^-})$ *and* $(\mathbf{U}_h^{\lambda},\zeta_+^{\lambda})$ *respectively in*

$$\Big(C(0,T;L^2(\omega^-,\mathbb{R}^2)\cap L^2(0,T;H^1(\omega^-,\mathbb{R}^2))\Big)\times\Big(L^2(\omega^-\times(0,T))\cap C(0,T;L^2(\omega^-))\Big)$$

and

$$\Big(C(0,T;L^2(\Omega^+,\mathbb{R}^2)\cap L^2(0,T;H^1(\Omega^+,\mathbb{R}^2))\Big)\times\Big(L^2(\omega^+\times(0,T))\cap C(0,T;L^2(\omega^+))\Big),$$

where $\mathbf{u}|_{\omega^-}$ *et* $\zeta|_{\omega^-}$ *denote the restriction in* ω^- *of* $(\mathbf{u},\zeta)$ *solution of the linearized shallow water system throughout the domain* ω*. The sequence of barotropic velocities* $(\overline{\mathbf{U}}_h^{k+1})_{k\geq 0}$ *and the sequence* $(\zeta_+^{k+1})_{k\geq 0}$ *converge repectively to* $\mathbf{u}|_{\omega^+}$ *and* $\zeta|_{\omega^+}$*. At convergence, the natural constraints* (2.24) *and* (2.25) *are satisfied.*

Proof. The convergence of the coupling algorithm results from Lemma 3.2.
The proof of the well-posedness of the two systems in Algorithms 1 and 2 is quite similar to the one given in [3] and [6]. We will only give here its outline.
For $\mathbf{U}_h^0$ and ζ_+^0 given and for all $k\geq 0$, the proof of the well-posedness of the coupling Algorithm 1 is equivalent to the proof of the well-posedness of the following systems with the prescribed Dirichlet boundary conditions $\overline{\mathbf{U}}_-^d$, ζ_-^d, $\mathbf{U}_+^d$ and ζ_+^d respectively on $\partial\omega_{out}^-\times(0,T)$, $\partial\omega_{out}^-\times(0,T)$, $(\partial\Omega_{out}^+\setminus\Gamma_B\cup\Gamma_T)\times(0,T)$ and $\partial\omega_{out}^+\times(0,T)$:

- In the domain ω^-, we solve the parabolic system:

$$\begin{cases} \partial_t\mathbf{u}^{k+1}+(\mathbf{U}_0.\nabla_h)\mathbf{u}^{k+1}-\mu\Delta_h\mathbf{u}^{k+1}=-g\nabla_h\zeta_-^{k+1} & \text{in } \omega^-\times(0,T) & \text{(3.9a)}\\ \mathcal{B}_-(\mathbf{u}^{k+1},\zeta_-^{k+1})=\mathcal{B}_-(\overline{\mathbf{U}}_h^k,\zeta_+^k) & \text{on } \gamma\times(0,T) & \text{(3.9b)}\\ \mathbf{u}^{k+1}(\,\cdot\,,0)=\overline{\mathbf{U}}_-^{ini} & \text{in } \omega^- & \text{(3.9c)}\end{cases}$$

  and the transport equation:

$$\begin{cases} \partial_t\zeta_-^{k+1}+\mathbf{U}_0.\nabla_h\zeta_-^{k+1}=-H\ \mathrm{div}_h(\mathbf{u}^{k+1}) & \text{in } \omega^-\times(0,T) & \text{(3.10a)}\\ \zeta_-^{k+1}(\,\cdot\,,0)=\zeta_-^{ini} & \text{in } \omega^- & \text{(3.10b)}\end{cases}$$

  We do not consider here a boundary condition at $x=L_0=0$ for the transport equation as we assumed $u_0>0$.

- In the domain Ω^+, we solve the parabolic system:

$$\begin{cases} \partial_t\mathbf{U}_h^{k+1}+(\mathbf{U}_0.\nabla_h)\mathbf{U}_h^{k+1}-\mu\Delta_h\mathbf{U}_h^{k+1}=-g\nabla_h\zeta_+^{k+1} & \text{in } \Omega^+\times(0,T) & \text{(3.11a)}\\ \mu\partial_z\mathbf{U}_h^{k+1}=0 & \text{at } z=0 & \text{(3.11b)}\\ \mu\partial_z\mathbf{U}_h^{k+1}=0 & \text{at } z=-H & \text{(3.11c)}\\ \mathcal{B}_+^{\mathbf{u}}(\mathbf{U}_h^{k+1},\zeta_+^{k+1})=\mathcal{B}_+^{\mathbf{u}}(\mathbf{u}^{k+1},\zeta_-^{k+1}) & \text{on } \Gamma\times(0,T) & \text{(3.11d)}\\ \mathbf{U}_h^{k+1}(\,\cdot\,,0)=\mathbf{U}_+^{ini} & \text{in } \Omega^+ & \text{(3.11e)}\end{cases}$$

and the transport equation:

$$\begin{cases} \partial_t \zeta_+^{k+1} + \mathbf{U}_0.\nabla_h \zeta_+^{k+1} = -H\ \mathrm{div}_h(\overline{\mathbf{U}}_h^{k+1}) & \text{in } \omega^+ \times (0,T) \quad (3.12a) \\ \mathcal{B}_+^{\zeta}\Big(\mathbf{U}_h^{k+1}, \zeta_+^{k+1}\Big) = \mathcal{B}_+^{\zeta}\Big(\mathbf{u}^{k+1}, \zeta_-^{k+1}\Big) & \text{on } \gamma \times (0,T) \quad (3.12b) \\ \zeta_+^{k+1}(\,\cdot\,,0) = \zeta_+^{ini} & \text{in } \omega^+ \quad (3.12c) \end{cases}$$

where the operator $\mathcal{B}_+$ is split as $\mathcal{B}_+ = (\mathcal{B}_+^{\mathbf{u}}, \mathcal{B}_+^{\zeta})^T$ with

$$\mathcal{B}_+^{\mathbf{u}}(\mathbf{u},\zeta) = -\mu\frac{\partial \mathbf{u}}{\partial x} + g\begin{pmatrix} \zeta \\ 0 \end{pmatrix} + \frac{(\lambda + u_0)}{2}\mathbf{u} \quad \text{and} \quad \mathcal{B}_+^{\zeta}(\mathbf{u},\zeta) = u_0\zeta$$

Then we prove in each subdomain the well-posedness of the parabolic system with a prescribed water height and the transport equation with a prescribed velocity. Finally one can use the fixed point theorem to conclude that the Schwarz algorithm is well-posed (see [3] and [6] for further details). ■

4. Modeling error

Unlike the usual case of domain decomposition, at convergence of the Schwarz algorithm, we do not have $\mathbf{U}_h^{\lambda}$ the limit of $(\mathbf{U}_h^k)$ equal to $\mathbf{U}_{h|\Omega^+}^G$, where $\mathbf{U}_h^G$ is the solution of system (2.7).

Due to the way the coupling algorithm is rewritten, the error is obviously contained in the baroclinic velocity. We will thus investigate, as in [29], the amplitude of the modeling error between the baroclinic velocity $\mathbf{U}_b^{\lambda}$ of the coupled solution and the baroclinic velocity $\mathbf{U}_b^G = \mathbf{U}_h^G - \overline{\mathbf{U}}_h^G$ of the global reference solution. As in [29], the choice of Robin-like operators allows its control. Actually we have the following result:

Theorem 4.1. *For every $\lambda > 0$, let $\mathbf{U}_b^{\lambda}$ denote the sum of the baroclinic modes of the coupled solution. If $L_0 < L_1$, then there exists $M = M(\lambda)$ such that*

$$\|\mathbf{U}_h^G - \overline{\mathbf{U}}_h^G - \mathbf{U}_b^{\lambda}\|_{L^2((0,T);H^1(\Omega^+)} + \|\mathbf{U}_h^G - \overline{\mathbf{U}}_h^G - \mathbf{U}_b^{\lambda}\|_{C([0,T];L^2(\Omega^+)} \leq M(\lambda)\varepsilon\sqrt{1+\delta^2} \quad (4.1)$$

where $\delta = \frac{L_1}{L_1 - L_0}$

Proof. Let us introduce in the sequel the function $\mathbf{E}_+^{\lambda}$ defined by $\mathbf{E}_+^{\lambda} = \mathbf{U}_h^G - \overline{\mathbf{U}}_h^G - \mathbf{U}_b^{\lambda}$. Therefore $\mathbf{E}_+^{\lambda}$ is solution of the system:

$$\begin{cases} \dfrac{\partial \mathbf{E}_+^{\lambda}}{\partial t} + (\mathbf{U}_0.\nabla_h)\mathbf{E}_+^{\lambda} - \mu\Delta\mathbf{E}_+^{\lambda} = 0 & \text{in } \Omega^+ \times (0,T) \\ \mathcal{B}_+^{out}\Big(\mathbf{E}_+^{\lambda}\Big) = 0 & \text{in } \partial\Omega_{out}^+ \times (0,T) \\ \mathcal{B}'_+\Big(\mathbf{E}_+^{\lambda}\Big) = \mathcal{B}'_+(\mathbf{U}_h^G - \overline{\mathbf{U}}_h^G) & \text{on } \Gamma \times (0,T) \\ (\mathbf{E})_+^{\lambda}(\,\cdot\,,0) = 0 & \text{in } \Omega^+ \end{cases} \quad (4.2)$$

where $\mathbf{U}_0 = (u_0, v_0)$ with $u_0 > 0$ and the interface operator $\mathcal{B}'_+$ is defined by:

$$\mathcal{B}'_+(\mathbf{U}) = \begin{pmatrix} -\mu\dfrac{\partial U}{\partial x} + \dfrac{(\lambda+u_0)}{2}U \\ -\mu\dfrac{\partial V}{\partial x} + \dfrac{(\lambda+u_0)}{2}V \end{pmatrix}$$

where $\mathbf{U} = (U, V)$. Multiplying (4.2) by $\mathbf{E}_+^{\lambda}$ and integrating over Ω^+ leads to:

$$\int_{\Omega^+} \frac{\partial \mathbf{E}_+^{\lambda}}{\partial t}.\mathbf{E}_+^{\lambda} + \int_{\Omega^+} (\mathbf{U}_0.\nabla_h)\mathbf{E}_+^{\lambda}.\mathbf{E}_+^{\lambda} - \mu\int_{\Omega^+} \Delta\mathbf{E}_+^{\lambda}.\mathbf{E}_+^{\lambda} = 0 \quad (4.3)$$

Integrating by parts and using the following relation:

$$-\mu\int_{\Omega^+}\Delta\mathbf{E}_+^\lambda.\mathbf{E}_+^\lambda=\mu\int_{\Omega^+}\nabla_h\mathbf{E}_+^\lambda:\nabla_h\mathbf{E}_+^\lambda+\mu\int_{\Omega^+}\frac{\partial\mathbf{E}_+^\lambda}{\partial z}.\frac{\partial\mathbf{E}_+^\lambda}{\partial z}-\mu\int_\Gamma\frac{\partial\mathbf{E}_+^\lambda}{\partial\mathbf{n}^+}.\mathbf{E}_+^\lambda$$

where $\mathbf{n}^+=(n_1^+,n_2^+,n_3^+)^T$ denotes the unit outward vector normal to Ω^+, equation (4.3) then becomes:

$$\frac{1}{2}\frac{\mathrm{d}}{\mathrm{d}t}\left\|\mathbf{E}_+^\lambda\right\|_{\Omega^+}^2+\int_{\Omega^+}(\mathbf{U}_0.\nabla_h)\mathbf{E}_+^\lambda.\mathbf{E}_+^\lambda+\mu\left\|\nabla_h\mathbf{E}_+^\lambda\right\|_{\Omega^+}^2+\mu\left\|\frac{\partial\mathbf{E}_+^\lambda}{\partial z}\right\|_{\Omega^+}^2-\mu\int_\Gamma\frac{\partial\mathbf{E}_+^\lambda}{\partial\mathbf{n}^+}.\mathbf{E}_+^\lambda=0$$

Now, one has:

$$\int_{\Omega^+}(\mathbf{U}_0.\nabla_h)\mathbf{E}_+^\lambda.\mathbf{E}_+^\lambda=-\int_{\Omega^+}(\mathbf{U}_0.\nabla_h)\mathbf{E}_+^\lambda.\mathbf{E}_+^\lambda+\int_\Gamma u_0\mathbf{E}_+^\lambda.\mathbf{E}_+^\lambda n_1^+ +\int_\Gamma v_0\mathbf{E}_+^\lambda.\mathbf{E}_+^\lambda n_2^+$$

and as $\mathbf{n}^+=(-1,0,0)$, this implies:

$$\int_{\Omega^+}(\mathbf{U}_0.\nabla_h)\mathbf{E}_+^\lambda.\mathbf{E}_+^\lambda=-\frac{1}{2}\int_\Gamma u_0\mathbf{E}_+^\lambda.\mathbf{E}_+^\lambda n_1^+$$

Equation (4.3) leads to:

$$\frac{1}{2}\frac{\mathrm{d}}{\mathrm{d}t}\left\|\mathbf{E}_+^\lambda\right\|_{\Omega^+}^2+\mu\left\|\nabla_h\mathbf{E}_+^\lambda\right\|_{\Omega^+}^2+\mu\left\|\frac{\partial\mathbf{E}_+^\lambda}{\partial z}\right\|_{\Omega^+}^2=\int_\Gamma\left(\frac{1}{2}u_0\mathbf{E}_+^\lambda-\mu\frac{\partial\mathbf{E}_+^\lambda}{\partial x}\right).\mathbf{E}_+^\lambda$$

Due to the boundary condition on Γ, one has:

$$\frac{1}{2}\frac{\mathrm{d}}{\mathrm{d}t}\left\|\mathbf{E}_+^\lambda\right\|_{\Omega^+}^2+\mu\left\|\nabla_h\mathbf{E}_+^\lambda\right\|_{\Omega^+}^2+\mu\left\|\frac{\partial\mathbf{E}_+^\lambda}{\partial z}\right\|_{\Omega^+}^2=\int_\Gamma\left(\mathcal{B}'_+(\mathbf{E}_+^\lambda)-\frac{\lambda}{2}\mathbf{E}_+^\lambda\right).\mathbf{E}_+^\lambda$$

and therefore:

$$\frac{1}{2}\frac{\mathrm{d}}{\mathrm{d}t}\left\|\mathbf{E}_+^\lambda\right\|_{\Omega^+}^2+\mu\left\|\nabla_h\mathbf{E}_+^\lambda\right\|_{\Omega^+}^2+\mu\left\|\frac{\partial\mathbf{E}_+^\lambda}{\partial z}\right\|_{\Omega^+}^2+\frac{\lambda}{2}\left\|\mathbf{E}_+^\lambda\right\|_\Gamma^2=\int_\Gamma\mathcal{B}'_+(\mathbf{E}_+^\lambda).\mathbf{E}_+^\lambda \tag{4.4}$$

The right-hand side of equation (4.4) reads as follows (since $\mathcal{B}'_+(\mathbf{U}_b^\lambda)=0$):

$$\int_\Gamma\mathcal{B}'_+(\mathbf{E}_+^\lambda).\mathbf{E}_+^\lambda=\int_\Gamma\mathcal{B}'_+(\mathbf{U}_h^G-\overline{\mathbf{U}}_h^G).\left(\mathbf{U}_h^G-\overline{\mathbf{U}}_h^G-\mathbf{U}_b^\lambda\right) \tag{4.5}$$

$$=\int_\Gamma\mathcal{B}'_+(\mathbf{U}_h^G-\overline{\mathbf{U}}_h^G).\left(\mathbf{U}_h^G-\overline{\mathbf{U}}_h^G\right)-\int_\Gamma\mathcal{B}'_+(\mathbf{U}_h^G-\overline{\mathbf{U}}_h^G).\overline{\mathbf{U}}_b^\lambda \tag{4.6}$$

Due to the relations (2.16) and (2.17), one has:

$$\mathbf{U}_h^G-\overline{\mathbf{U}}_h^G=O(\varepsilon^2)$$

Then, due again to the relations (2.16) and (2.17), it is reasonable to assume that $\mathcal{B}'_+(\mathbf{U}_h^G-\overline{\mathbf{U}}_h^G)=O(1)$, so that one has:

$$\int_\Gamma\mathcal{B}'_+(\mathbf{U}_h^G-\overline{\mathbf{U}}_h^G).\left(\mathbf{U}_h^G-\overline{\mathbf{U}}_h^G\right)=O(\varepsilon^2)$$

Now we will focus on the term $\int_\Gamma\mathcal{B}'_+(\mathbf{U}_h^G-\overline{\mathbf{U}}_h^G).\overline{\mathbf{U}}_b^\lambda$. In the same way and as in [29], if we assume that $L_0<L_1$, so that the 3D effects are insignificant in $\Omega^+\cap\{L_0\le x\le L_1\}$, and applying a similar asymptotic analysis as in the first section to the 3D model, we can deduce:

$$\mathbf{U}_h^\lambda=\overline{\mathbf{U}}_h^\lambda+O(\varepsilon'^2)$$

where $\varepsilon'=\frac{H}{L_1-L_0}=\frac{L_1}{L_1-L_0}\varepsilon$. We denote in the sequel $\delta=\frac{L_1}{L_1-L_0}$, therefore:

$$\mathbf{U}_b^\lambda=\mathbf{U}_h^\lambda-\overline{\mathbf{U}}_h^\lambda=O(\delta^2\varepsilon^2)$$

So that, there exists a positive constant C_1 depending continuously on λ and t such that:

$$\frac{1}{2}\frac{\mathrm{d}}{\mathrm{d}t}\left\|\mathbf{E}_+^\lambda\right\|_{\Omega^+}^2+\mu\left\|\nabla_h\mathbf{E}_+^\lambda\right\|_{\Omega^+}^2+\mu\left\|\frac{\partial\mathbf{E}_+^\lambda}{\partial z}\right\|_{\Omega^+}^2+\frac{\lambda}{2}\left\|\mathbf{E}_+^\lambda\right\|_\Gamma^2\le C_1(1+\delta^2)\varepsilon^2 \tag{4.7}$$

Integrating between 0 and t for $t \in [0;T]$ and using the initial conditions, (4.7) leads to:

$$\frac{1}{2}\left\|\mathbf{E}_+^\lambda\right\|_{\Omega^+}^2 + \mu\int_0^t \left\|\nabla_h \mathbf{E}_+^\lambda\right\|_{\Omega^+}^2 + \mu\int_0^t \left\|\frac{\partial \mathbf{E}_+^\lambda}{\partial z}\right\|_{\Omega^+}^2 + \frac{\lambda}{2}\int_0^t \left\|\mathbf{E}_+^\lambda\right\|_{\Gamma}^2 \leq C_2(\lambda,t)(1+\delta^2)\varepsilon^2 \tag{4.8}$$

and then (since $\mu > 0$ and $\lambda > 0$) one has:

$$\left\|\mathbf{E}_+^\lambda\right\|_{\Omega^+}^2 \leq 2C_2(\lambda,t)(1+\delta^2)\varepsilon^2 \tag{4.9}$$

and we can also deduce that:

$$\int_0^T \left\|\mathbf{E}_+^\lambda\right\|_{\Omega^+}^2 + \int_0^T \left\|\nabla \mathbf{E}_+^\lambda\right\|_{\Omega^+}^2 \leq C_3(\lambda)(1+\delta^2)\varepsilon^2 \tag{4.10}$$

Finally, we can establish the error majoration (4.1). ∎

Remark 4.2. Note that if we consider a bottom friction, as explained previously in Remark 2.5, Section 3.1 and Remark 3.3, Lemma 3.2 is no longer true as the two Algorithms 1 and 2 are no more equivalent. Besides, depending on the amplitude of the friction coefficient, the second order relation (2.10) has to be revised. Nevertheless, if the dimensionless friction amplitude K introduced in Remark 2.5 is small enough, that is $K = O(\varepsilon^2)$, one can deal directly with the Schwarz algorithm 1 with boundary conditions (3.6) and (3.8). As the systems remain of the same mathematical nature, the proof of the convergence of the Schwarz coupling algorithm 1 with the boundary conditions (3.6) and (3.8) should be similar to the proof of the convergence of the classical domain decomposition algorithm of shallow water equations with boundary conditions (3.6) and (3.7) established in [6]. In this case, Theorem 4.1 has to be revisited by comparing the restriction of the global solution to the domain Ω^+ with the 3D part of the coupled solution. Now, if we assume that $K = O(\varepsilon)$, one has to consider the appropriate second order shallow water system as explained in Remark 2.5 and to deal with a parabolic distribution throughout the interface Γ. This implies a new definition of the extension operator $\mathcal{E}$. The main results of this work and of the related work [6], i.e. the well-posedness and the convergence of the algorithm 1 and the control of the modeling error, have then to be revised in order to take in account this new extension operator.

5. Numerical schemes and tests

The aim of this section is to illustrate the previous theoretical results with some numerical experiments. In a first step and to illustrate the theoretical convergence result of the Schwarz coupling algorithm, we study the numerical convergence of the domain decomposition method applied to the shallow water equations. Then, in a second step, experiments with the dimensionally heterogeneous coupling method are conducted. All the codes are available in [1].

5.1. Domain decomposition for the 2D shallow water equations

In this subsection, we numerically study the convergence of the domain decomposition method for 2D linearized shallow water equations. We first present the monodomain solution, i.e. the numerical solution to system (2.19) throughout the whole domain ω, and then we numerically set up the Schwarz algorithm and illustrate its convergence.

5.1.1. *Reference monodomain solution*

In this paragraph, we detail the parameters of the numerical monodomain configuration and the resulting simulated solution. This reference solution will allow to quantify the convergence of the domain decomposition algorithm.

Domain and boundary conditions. The 2D linearized shallow water equations are solved in $\omega = [-L; L] \times [0; L_y]$. Although the mathematical analysis has been developed with a null right-hand side, we consider for the numerical tests a non-zero source term $\tau = (\tau_x, 0)^T$ (wind stress) (this does not change the theoretical convergence results, since the proofs concern the errors at each iteration, not the solutions). We impose also homogeneous Dirichlet conditions for the velocity $\mathbf{u}$ and for the water height ζ on the boundary $\partial\omega$.

Numerical schemes. Model equations are discretized using a finite difference scheme on a $2N_x \times N_y$ cartesian staggered Arakawa C-grid [2] (velocities are computed on the edges of each cell and water height in the center – see Figure 5.1). The space steps are $\Delta x = \frac{L}{N_x}$ and $\Delta y = \frac{L_y}{N_y}$. For $0 \leq i \leq 2N_x$ and $0 \leq j \leq N_y$, the cell $C_{i,j}$ is defined by $C_{i,j} = [x_i; x_{i+1}] \times [y_j; y_{j+1}]$, where $x_i = -L + i\Delta x$ and $y_j = j\Delta y$. We define also a time step $\Delta t = \frac{T}{N_t}$, and $t_n = n\Delta t$ for $0 \leq n \leq N_t$. The discrete unknowns are $u^n_{i,j} \simeq u(x_i, y_j, t_n)$, $v^n_{i,j} \simeq v(x_{i+\frac{1}{2}}, y_{j+\frac{1}{2}}, t_n)$ and $\zeta^n_{i,j} \simeq \zeta(x_{i+\frac{1}{2}}, y_j, t_n)$.

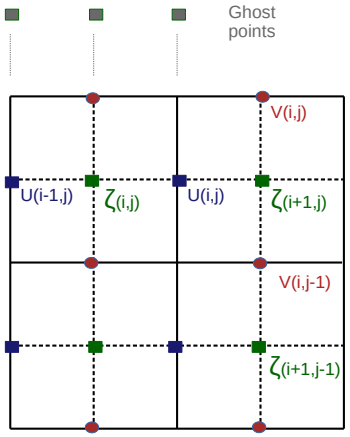

FIGURE 5.1. Staggered grid in space

- The equation for u

$$\frac{\partial u}{\partial t} + u_0 \frac{\partial u}{\partial x} + v_0 \frac{\partial u}{\partial y} + g\frac{\partial \zeta}{\partial x} = \mu\left(\frac{\partial^2 u}{\partial x^2} + \frac{\partial^2 u}{\partial y^2}\right) + \tau_x \tag{5.1}$$

is discretized using standard explicit schemes as follows:

$$\frac{1}{\Delta t}(u^{n+1}_{i,j} - u^n_{i,j}) + \frac{u_0}{\Delta x}(u^n_{i,j} - u^n_{i-1,j}) + \frac{v_0}{2\Delta y}(u^n_{i,j+1} - u^n_{i,j-1}) + \frac{g}{\Delta x}(\zeta^n_{i,j} - \zeta^n_{i-1,j})$$
$$= \frac{\mu}{\Delta x}\left(\frac{\partial u}{\partial x}\right)^n_{i+1,j} - \frac{\mu}{\Delta x}\left(\frac{\partial u}{\partial x}\right)^n_{i,j} + \mu\frac{u^n_{i,j+1} - 2u^n_{i,j} + u^n_{i,j-1}}{\Delta y^2} + (\tau_x)_{i,j} \tag{5.2}$$

Note that the discretization of $\partial^2 u/\partial x^2$ can also be written as

$$\frac{u^n_{i+1,j} - 2u^n_{i,j} + u^n_{i-1,j}}{\Delta x^2} = \frac{1}{\Delta x}\left(\left(\frac{\partial u}{\partial x}\right)^n_{i+1,j} - \left(\frac{\partial u}{\partial x}\right)^n_{i,j}\right) \tag{5.3}$$

where $\left(\frac{\partial u}{\partial x}\right)^n_{i,j} = \frac{u^n_{i,j} - u^n_{i-1,j}}{\Delta x} \simeq \frac{\partial u}{\partial x}(t_n, x_i, y_j)$. This will be used later for the discretization of the Schwarz algorithm.

- Similarly the equation for v

$$\frac{\partial v}{\partial t} + u_0 \frac{\partial v}{\partial x} + v_0 \frac{\partial v}{\partial y} + g \frac{\partial \zeta}{\partial y} = \mu \left(\frac{\partial^2 v}{\partial x^2} + \frac{\partial^2 v}{\partial y^2} \right) \tag{5.4}$$

is discretized as

$$\begin{aligned} \frac{1}{\delta t}(v_{i,j}^{n+1} - v_{i,j}^n) + \frac{u_0}{\Delta x}(v_{i,j}^n - v_{i-1,j}^n) + \frac{v_0}{2\Delta y}(v_{i,j+1}^n - v_{i,j-1}^n) + \frac{g}{2\Delta y}(\zeta_{i,j+1}^n - \zeta_{i,j-1}^n) \\ = \frac{\mu}{\Delta x}\left(\frac{\partial v}{\partial x}\right)_{i+1,j}^n - \frac{\mu}{\Delta x}\left(\frac{\partial v}{\partial x}\right)_{i,j}^n + \mu \frac{v_{i,j+1}^n - 2v_{i,j}^n + v_{i,j-1}^n}{\Delta y^2} \end{aligned} \tag{5.5}$$

- Finally, the discrete equation for ζ is:

$$\begin{aligned} \frac{1}{\delta t}(\zeta_{i,j}^{n+1} - \zeta_{i,j}^n) + \frac{H}{\Delta x}(u_{i,j}^n - u_{i-1,j}^n) + \frac{H}{\Delta y}(v_{i,j}^n - v_{i,j-1}^n) \\ + \frac{u_0}{2\Delta x}(\zeta_{i+1,j}^n - \zeta_{i-1,j}^n) + \frac{v_0}{2\Delta y}(\zeta_{i,j+1}^n - \zeta_{i,j-1}^n) = 0 \end{aligned} \tag{5.6}$$

Note that actual schemes in realistic models are of course more sophisticated (e.g. property preserving, higher order, etc.).

Monodomain reference solution. For this reference simulation, we choose a 300 m × 100 m rectangular basin and $T = 5$ seconds. The other physical parameters of the simulation are detailed in the following table:

Δx	Δy	Δt	μ	u_0	v_0
1.2 m	1.0 m	0.001 s	30 $\mathrm{m}^2/\mathrm{s}^{-1}$	1.02 m/s	1.02 m/s

Regarding the term source and the initial velocity, we choose $\tau_x(x, y) = \tau_0 \sin\left(\frac{\pi}{L_y} y\right)$ with $\tau_0 = 1\,\mathrm{ms}^{-2}$ and the simulation is started at rest. That is $\mathbf{u}(\,\cdot\,, 0) = (0, 0)^T$. The simulation lasts for 5 seconds. The zonal velocity u of this reference solution at $t = 5$ seconds is displayed in Figure 5.2.

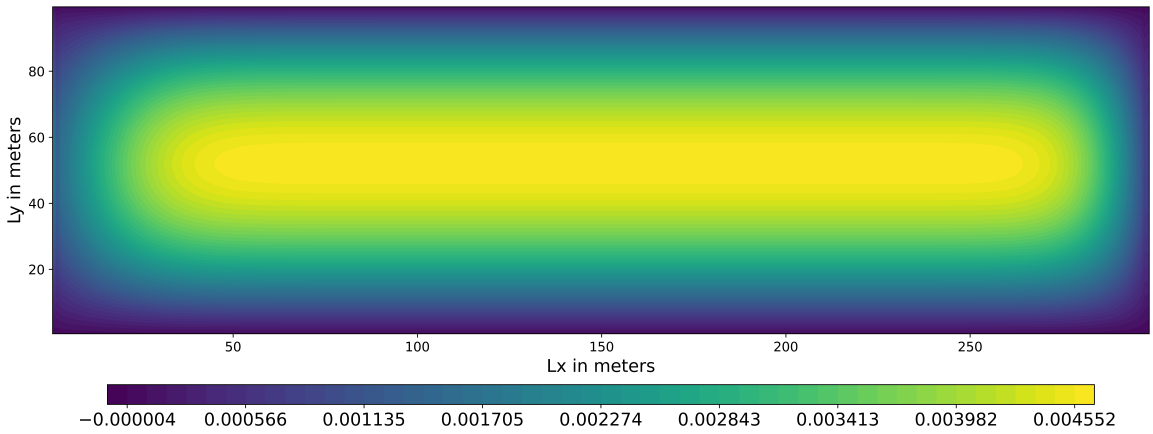

Figure 5.2. Zonal velocity u of the reference monodomain solution at $t = 5$ s.

5.1.2. *Numerical scheme for the domain decomposition algorithm*

We now numerically study the domain decomposition algorithm (3.4) and (3.5) with Robin-like boundary conditions at the interface. Let split $\omega = [-L; L] \times [0; L_y]$ into two non-overlapping subdomains $\omega^- = [-L; 0] \times [0; L_y]$ and $\omega^+ = [0; L] \times [0; L_y]$. Boundary conditions for $(u,\, v,\, \zeta)$ are exchanged at the interface γ located at $x = 0$. The grids of ω^- and ω^+ have both $N_x \times N_y$ cells. As the grids are staggered, the physical boundary along the y-axis (western portion $x = -L$ and eastern portion $x = L$) is located on u-points, while it is located on v-points along the x-axis (southern portion $y = 0$ and northern portion $y = L_y$), resulting in the need for ghost points for the other variables.

For the subdomain ω^- (the discretization is similar in ω^+), and at each iteration k of the Schwarz algorithm, one has to solve the following problem:

$$\begin{cases} \mathcal{L}_{LSW}\Big(\mathbf{u}_-^{k+1}, \zeta_-^{k+1}\Big) = \tau & \text{in } (\omega^- \times (0,T))^2 \\ \mathcal{B}_-^{out}\Big(\mathbf{u}_-^{k+1}, \zeta_-^{k+1}\Big) = \overline{G}_-^{out} & \text{on } (\partial\omega_{out}^- \times (0,T))^2 \\ \mathcal{B}_-\Big(\mathbf{u}_-^{k+1}, \zeta_-^{k+1}\Big) = \mathcal{B}_-\Big(\mathbf{u}_+^{k}, \zeta_+^{k}\Big) & \text{on } (\gamma \times (0,T))^2 \\ \Big(\mathbf{u}_-^{k+1}, \zeta_-^{k+1}\Big)(\,\cdot\,, 0) = \Big(\overline{\mathbf{U}}_-^{ini}, \zeta_-^{ini}\Big) & \text{in } \omega^- \end{cases}$$

As in [21], we focus on two key points: the discretization of the boundary condition $\mathcal{B}_-(\mathbf{u}_-, \zeta_-) = \mathbf{G}$ for a given $\mathbf{G}$, and the extraction of the quantity $\mathcal{B}_-\Big(\mathbf{u}_+^{k}, \zeta_+^{k}\Big)$ from ω^+.

Recall that the transmission condition on γ reads:

$$\begin{cases} \mu\dfrac{\partial u_-^{k+1}}{\partial x} - g\,\zeta_-^{k+1} + \dfrac{1}{2}(\lambda - u_0)\,u_-^{k+1} = \mu\dfrac{\partial u_+^{k}}{\partial x} - g\,\zeta_+^{k} + \dfrac{1}{2}(\lambda - u_0)\,u_+^{k} \\ \mu\dfrac{\partial v_-^{k+1}}{\partial x} + \dfrac{1}{2}(\lambda - u_0)\,v_-^{k+1} = \mu\dfrac{\partial v_+^{k}}{\partial x} + \dfrac{1}{2}(\lambda - u_0)\,v_+^{k} \end{cases} \tag{5.7}$$

The discrete value of u and v at the interface γ should satisfy simultaneously this transmission condition and the discrete interior equations for u and v.

Let consider the discretization of the first equation of (5.7):

$$\mu\Big(\frac{\partial u_-}{\partial x}\Big)_{N_x,j}^{k+1,n} - g\,\zeta_{-,N_x,j}^{k+1,n} + \frac{1}{2}(\lambda - u_0)\,u_{-,N_x,j}^{k+1,n} = \mu\Big(\frac{\partial u_+}{\partial x}\Big)_{0,j}^{k,n} - g\,\zeta_{+,0,j}^{k,n} + \frac{1}{2}(\lambda - u_0)\,u_{+,0,j}^{k,n}$$

We note that the first two terms on the left hand-side are present in the discrete equation for u (5.2). We then isolate those two terms:

$$\mu\Big(\frac{\partial u_-}{\partial x}\Big)_{N_x,j}^{k+1,n} - g\,\zeta_{-,N_x,j}^{k+1,n} = A_+^k - \frac{1}{2}(\lambda - u_0)\,u_{-,N_x,j}^{k+1,n} \tag{5.8}$$

where A_+^k denotes the right-hand side of the first equation of (5.7), i.e. all the terms depending on u_+^k. The main objective in the sequel is to identify A_+^k in the discrete equation for u in ω^- and then to extract it from the model defined in ω^+.

From the discrete interior equation for u in ω^-, we deduce:

$$\begin{aligned} &\frac{1}{\Delta t}\Big(u_{-,N_x,j}^{k+1,n+1} - u_{-,N_x,j}^{k+1,n}\Big) + \frac{u_0}{\Delta x}\Big(u_{-,N_x,j}^{k+1,n} - u_{-,N_x-1,j}^{k+1,n}\Big) + \frac{v_0}{2\Delta y}\Big(u_{-,N_x,j+1}^{k+1,n} - u_{-,N_x,j-1}^{k+1,n}\Big) \\ &\quad - \frac{g}{\Delta x}\zeta_{-,N_x-1,j}^{k+1,n} + \frac{\mu}{\Delta x}\Big(\frac{\partial u_-}{\partial x}\Big)_{N_x-1,j}^{k+1,n} - \mu\frac{u_{-,N_x,j+1}^{k+1,n} - 2u_{-,N_x,j}^{k+1,n} + u_{-,N_x,j-1}^{k+1,n}}{\Delta y^2} - (\tau_x)_{N_x,j} \\ &\qquad = \frac{\mu}{\Delta x}\Big(\frac{\partial u_-}{\partial x}\Big)_{N_x,j}^{k+1,n} - \frac{g}{\Delta x}\zeta_{-,N_x,j}^{k+1,n} \end{aligned} \tag{5.9}$$

Therefore, we replace the right-hand side by (5.8):

$$\frac{1}{\Delta t}\Big(u^{k+1,n+1}_{-,N_x,j}-u^{k+1,n}_{-,N_x,j}\Big)+\frac{u_0}{\Delta x}\Big(u^{k+1,n}_{-,N_x,j}-u^{k+1,n}_{-,N_x-1,j}\Big)+\frac{v_0}{2\Delta y}\Big(u^{k+1,n}_{-,N_x,j+1}-u^{k+1,n}_{-,N_x,j-1}\Big)$$
$$-\frac{g}{\Delta x}\zeta^{k+1,n}_{-,N_x-1,j}+\frac{\mu}{\Delta x}\left(\frac{\partial u_-}{\partial x}\right)^{k+1,n}_{N_x-1,j}-\mu\frac{u^{k+1,n}_{-,N_x,j+1}-2u^{k+1,n}_{-,N_x,j}+u^{k+1,n}_{-,N_x,j-1}}{\Delta y^2}-(\tau_x)_{N_x,j}$$
$$=\frac{A^k_+}{\Delta x}-\frac{1}{2\Delta x}(\lambda-u_0)u^{k+1,n}_{-,N_x,j}\quad(5.10)$$

The next step consists in extracting A^k_+ from the model defined in ω^+. We have:

$$\frac{A^k_+}{\Delta x}=\frac{\mu}{\Delta x}\left(\frac{\partial u_+}{\partial x}\right)^{k,n}_{0,j}-\frac{g}{\Delta x}\zeta^{k,n}_{+,0,j}+\frac{1}{2\Delta x}(\lambda-u_0)u^{k,n}_{+,0,j}\quad(5.11)$$

The equation for u in ω^+ at iteration k of the Schwarz algorithm and at the interface γ reads:

$$\frac{1}{\Delta t}\Big(u^{k,n+1}_{+,0,j}-u^{k,n}_{+,0,j}\Big)+\frac{u_0}{\Delta x}\Big(u^{k,n}_{+,1,j}-u^{k,n}_{+,0,j}\Big)+\frac{v_0}{2\Delta y}\Big(u^{k,n}_{+,0,j+1}-u^{k,n}_{+,0,j-1}\Big)$$
$$+\frac{g}{\Delta x}\Big(\zeta^{k,n}_{+,1,j}-\zeta^{k,n}_{+,0,j}\Big)-(\tau_x)_{0,j}-\mu\frac{\Big(u^{k,n}_{+,0,j+1}-2u^{k,n}_{+,0,j}+u^{k,n}_{+,0,j-1}\Big)}{\Delta y^2}$$
$$=\frac{\mu}{\Delta x}\left(\frac{\partial u^k}{\partial x}\right)^n_{+,1,j}-\frac{\mu}{\Delta x}\left(\frac{\partial u^k}{\partial x}\right)^n_{+,0,j}\quad(5.12)$$

We deduce then that:

$$\frac{\mu}{\Delta x}\left(\frac{\partial u^k}{\partial x}\right)^n_{+,0,j}-\frac{g}{\Delta x}\zeta^{k,n}_{+,0,j}$$
$$=-\frac{1}{\Delta t}\Big(u^{k,n+1}_{+,0,j}-u^{k,n}_{+,0,j}\Big)-\frac{u_0}{\Delta x}\Big(u^{k,n}_{+,1,j}-u^{k,n}_{+,0,j}\Big)+\mu\frac{\Big(u^{k,n}_{+,0,j+1}-2u^{k,n}_{+,0,j}+u^{k,n}_{+,0,j-1}\Big)}{\Delta y^2}$$
$$-\frac{v_0}{2\Delta y}(u^{k,n}_{+,0,j+1}-u^{k,n}_{+,0,j-1})-\frac{g}{\Delta x}\zeta^{k,n}_{+,1,j}+\frac{\mu}{\Delta x}\left(\frac{\partial u^k}{\partial x}\right)^n_{+,1,j}+(\tau_x)_{0,j}\quad(5.13)$$

and then we have:

$$\frac{A^k_+}{\Delta x}=\frac{1}{2\Delta x}(\lambda-u_0)u^{k,n}_{+,0,j}-\frac{1}{\Delta t}\Big(u^{k,n+1}_{+,0,j}-u^{k,n}_{+,0,j}\Big)$$
$$-\frac{u_0}{\Delta x}\Big(u^{k,n}_{+,1,j}-u^{k,n}_{+,0,j}\Big)-\frac{v_0}{2\Delta y}\Big(u^{k,n}_{+,0,j+1}-u^{k,n}_{+,0,j-1}\Big)$$
$$+\mu\frac{\Big(u^{k,n}_{+,0,j+1}-2u^{k,n}_{+,0,j}+u^{k,n}_{+,0,j-1}\Big)}{\Delta y^2}-\frac{g}{\Delta x}\zeta^{k,n}_{+,1,j}+\frac{\mu}{\Delta x}\left(\frac{\partial u^k}{\partial x}\right)^n_{+,1,j}+(\tau_x)_{0,j}\quad(5.14)$$

Substituting A_+^k in (5.10), we obtain the final discrete equation for u in ω^-:

$$\begin{aligned}
&\frac{1}{\Delta t}\left(u_{-,N_x,j}^{k+1,n+1}-u_{-,N_x,j}^{k+1,n}\right)+\frac{u_0}{\Delta x}\left(u_{-,N_x,j}^{k+1,n}-u_{-,N_x-1,j}^{k+1,n}\right)+\frac{v_0}{2\Delta y}\left(u_{-,N_x,j+1}^{k+1,n}-u_{-,N_x,j-1}^{k+1,n}\right)\\
&\qquad-\frac{g}{\Delta x}\zeta_{-,N_x-1,j}^{k+1,n}+\frac{\mu}{\Delta x}\left(\frac{\partial u_-}{\partial x}\right)_{N_x-1,j}^{k+1,n}-\mu\frac{u_{-,N_x,j+1}^{k+1,n}-2u_{-,N_x,j}^{k+1,n}+u_{-,N_x,j-1}^{k+1,n}}{\Delta y^2}-(\tau_x)_{N_x,j}\\
&=-\frac{1}{2\Delta x}(\lambda-u_0)u_{-,N_x,j}^{k+1,n}+\frac{1}{2\Delta x}(\lambda-u_0)u_{+,0,j}^{k,n}-\frac{1}{\Delta t}\left(u_{+,0,j}^{k,n+1}-u_{+,0,j}^{k,n}\right)\\
&\qquad-\frac{u_0}{\Delta x}\left(u_{+,1,j}^{k,n}-u_{+,0,j}^{k,n}\right)+\mu\frac{\left(u_{+,0,j+1}^{k,n}-2u_{+,0,j}^{k,n}+u_{+,0,j-1}^{k,n}\right)}{\Delta y^2}
\end{aligned}\tag{5.15}$$

Note that the discretization of the equations in ω^+ and of the boundary condition $\mathcal{B}^+$ is similar to the previous calculations. The additional (third) component of $\mathcal{B}^+$ implies a Dirichlet–Dirichlet transmission condition: no special treatment is then needed.

5.1.3. *Numerical results*

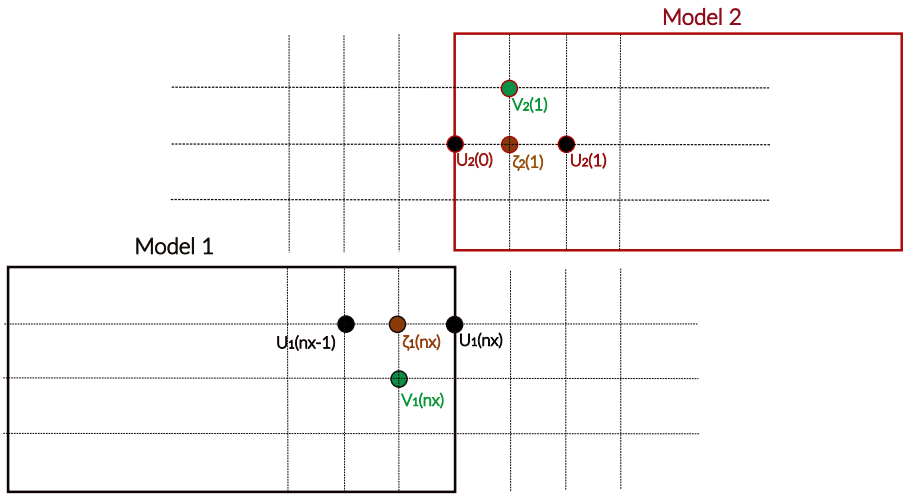

FIGURE 5.3. Configuration of the splitted domain

We split the channel into two subdomains of similar dimensions (Figure 5.3), and implement the discrete domain decomposition algorithm described in the previous paragraph. In order to avoid heavy computations by solving the algorithm over a long time interval, and because Schwarz algorithm is more efficient on small windows, we decompose the time interval $(0,T)$, where $T=5$ seconds, into P windows of equal lengths, as in [3] and [21]. In this experiment, we split the whole time interval into 16 windows of 100 time steps each. Since the aim of this numerical test is to validate the convergence of the decomposition domain algorithm for any $\lambda>0$, Figure 5.4(a) displays the relative L^2 norm $\frac{\|u-u^k\|_{L^2(\omega^+\times(0,T))}}{\|u\|_{L^2(\omega^+\times(0,T))}}$, integrated in time over the period, of the difference between the solution of the eastern model and the corresponding reference solution as a function of the Schwarz iteration k, for different values of λ. We can see that the algorithm converges but this convergence is very slow. In fact, a kind of saturation can be observed after a few iterations of the domain decomposition algorithm and the errors are of the order of 10^{-3}. This slow convergence and this error order are similar to those obtained in [21] in the case of a non-overlapping algorithm. As mentioned in this work, an

overlapping of one grid point could accelerate the convergence for a low extra cost. We do not test this possibility in the present work. We also notice that some "extremal" values of λ imply a very slow convergence (e.g. for $\lambda > 100$) of the algorithm. This is because such values make the algorithm behave like a non-overlapping domain decomposition algorithm with almost "Dirichlet–Dirichlet" or "Neumann–Neumann" interface conditions. We also show in Figure 5.4(b) the L^2 norm of the error at the iteration 19 of the algorithm as a function of λ. The numerical results suggest that some values of λ give a better convergence of the algorithm. One can then numerically optimize the rate of the convergence.

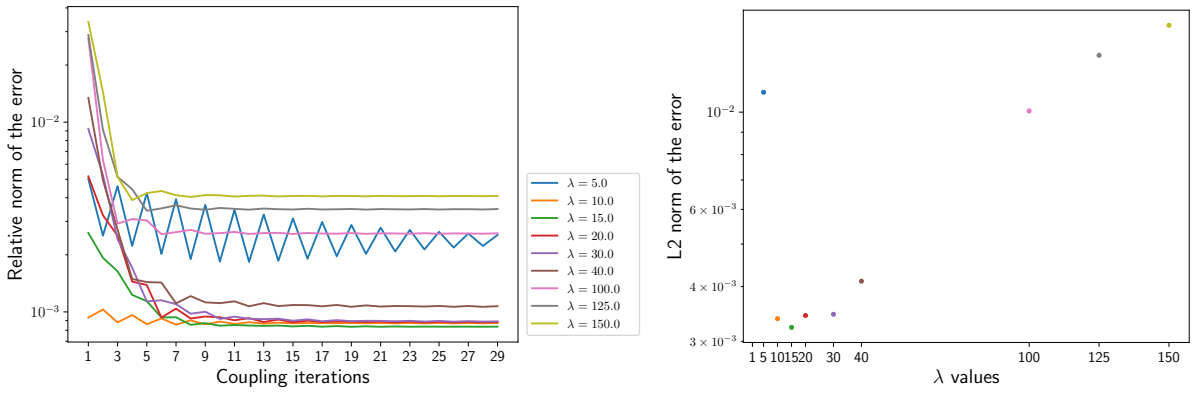

(A) (B)

Figure 5.4. Left panel: Relative L^2 norm of the error as a function of the iteration index, for several values of λ. Right panel: L^2 norm of the error at iteration $k = 19$ for different values of λ

5.2. Coupling hydrostatic linearized Navier–Stokes system with corresponding linearized shallow water system

First, let us note that for the sake of simplicity, and since the boundary conditions (3.6) and (3.8) do not depend on y, we will numerically illustrate the coupling of the one dimensional x version of (2.19) with the two dimensional (x, z) version of (2.20). We do not detail the discretization of the models and of the interface boundary conditions, since it is quite similar to the discretization of the linearized shallow water equations.

5.2.1. *Reference monodomain global solution*

In this paragraph we detail the parameters of the numerical global solution. This reference solution will enable the modeling error made to be quantified, as a function of the parameter λ and of the interface position. The numerical reference solution is obtained by solving the x-z version of the system (2.7) on the whole domain Ω.

Domain and boundary conditions. The numerical reference solution is obtained by solving the x-z version of the system (2.7) on the whole domain $\Omega = [-L; L] \times [-H; 0]$ with $\omega = [-L; L]$ then. As for the numerical monodomain solution of the Shallow Water system, a source term $\tau = (\tau_x, 0)^T$ is added. We impose homogeneous Dirichlet boundary conditions for the velocity $\mathbf{U}_h$ and for the water height ζ on the boundaries $\partial\Omega$ and $\partial\omega$. We start also from a non-zero initial velocity $\mathbf{U}_h^{ini} = (U^{ini}, 0)^T$.

Numerical reference global solution. The physical dimensions of the whole domain are $L = 200m$, and $H = 2m$. Consequently the ϵ parameter for the Navier–Stokes model is equal to 0.005. The other physical parameters of the simulation are detailed in the following table:

Δx	Δz	Δt	μ	u_0
0.5 m	0.1 m	0.0004 s	10 $\mathrm{m}^2/\mathrm{s}^{-1}$	1 m/s

Due to the explicit Euler time scheme discretization, the time-step is very small.

Regarding the term source and the initial velocity, we choose $\tau_x = m \exp\Big(-\frac{(x-x^*)^2}{D}\Big) \sin\big(2\pi \frac{z}{H}\big)$ where $m = 0.1ms^{-2}$, $D = 50$ and x^* located at around 93% of the whole domain length and $U^{ini} = m_i \exp\Big(-\frac{(x-x^*)^2}{D}\Big) \sin\big(2\pi \frac{z}{H}\big)$ with $m_i = 0.001ms^{-2}$. Figure 5.5 displays the numerical reference solution corresponding to (2.7) for different time steps. We can clearly see the vertical effects in the rightmost part of the domain, which persist over time.

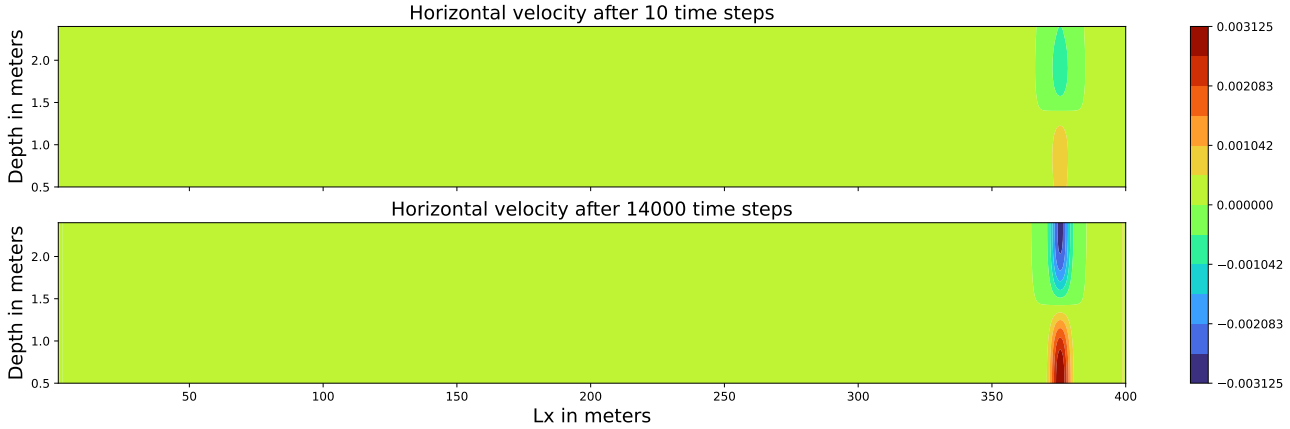

Figure 5.5. Horizontal velocity of the NS reference simulation after 10 (top) and 14000 (bottom) time steps.

5.2.2. *Numerical results of the coupling algorithm*

We now split the domain Ω into two subdomains of equal size, and in the left subdomain, we replace the x-z version of the linearized hydrostatic Navier–Stokes system (designed in the sequel by the NS model) by a x version of the linearized shallow water system (designed by the SW model) — see Figure 5.6. The discretization and the boundary conditions for both SW and NS models are calculated in the same way as in the domain decomposition method. In this experiment, we split the whole time interval into 9 windows of 2000 time steps each.

Convergence. Figure 5.7 presents the absolute and relative L^2 norms of the difference between the successive iterates of the Schwarz algorithm. We can see that the algorithm converges for the different tested values of λ. However the convergence is slow for some values of λ.

Sensitivity to the parameter λ. As mentioned and studied in Section 2.4, unlike the classical domain decomposition methods, the converged coupled solution is not equal to the restriction of the reference solution on each subdomain. In Theorem 4.1 we highlight a dependence of this modeling error with respect to λ, to ε and to the interface position. Figure 5.8 (a) illustrates this dependence w.r.t. λ. We can see that, for the values of λ leading to comparable rates of convergence of the coupling

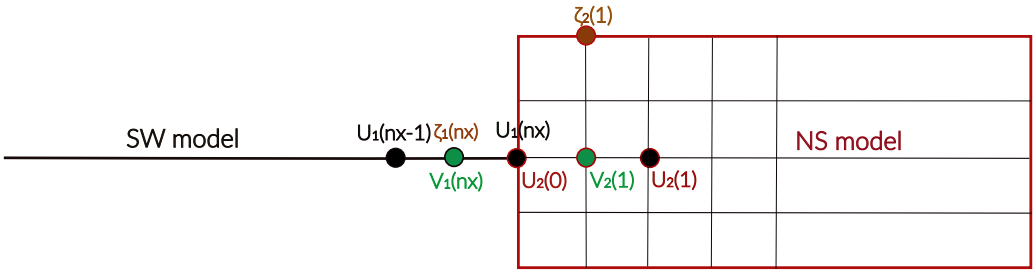

Figure 5.6. Grids of the 1D/2D domains

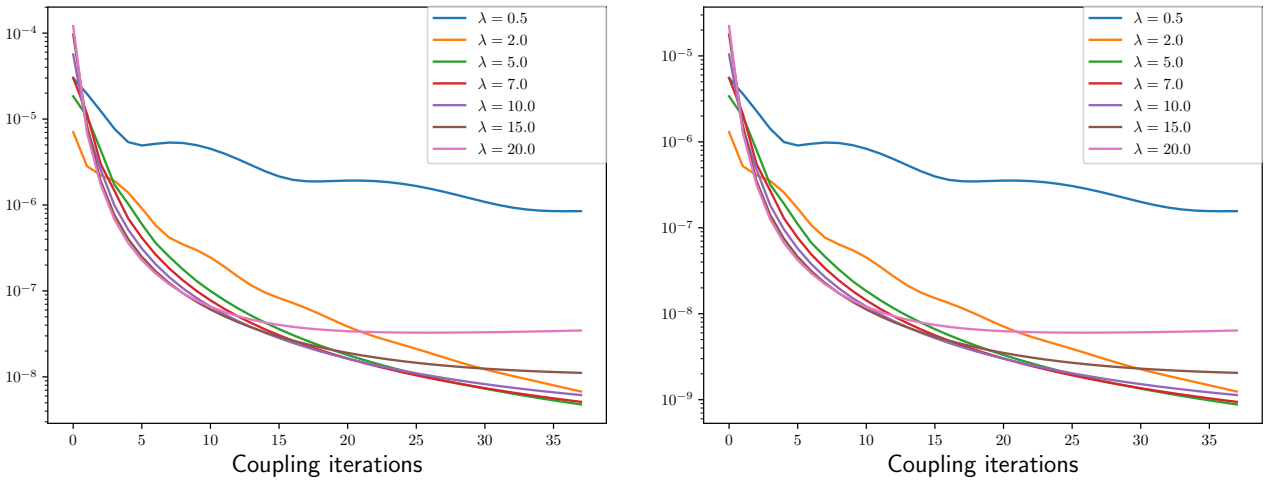

Figure 5.7. Left panel: L^2 norm of the difference between successive iterates $\|U^{k+1} - U^k\|_{\Omega^+ \times (0;T)}$ as a function of k. Right panel: corresponding relative L^2 norm $\frac{\|U^{k+1} - U^k\|_{L^2(\Omega^+ \times (0;T))}}{\|U^k\|_{L^2(\Omega^+ \times (0;T))}}$

algorithm (see Figure 5.7), this error remains of the order of 10^{-7} m.s^{-1} all along the coupling windows. Similarly to the numerical results obtained in [28] in the elliptic case, the amplitude of its variations in L^2 seems to not depend on λ.

Sensitivity to the interface position. We also performed experiments to illustrate the dependence of the modeling error on the interface position. We fixed the value of λ to 5, which leads to a good convergence rate and minimizes the modeling error (see Figures 5.7 and 5.8 (a)) and looked at the solution after 5, 10 and 40 iterations. We can see on Figure 5.8 (b) that the error regularly increases with the shift of the coupling interface. The error begins to increase significantly for an interface located around 85% of the entire 2D domain length, meaning that the global solution changes from 1D to 2D behavior. This is consistent with the expression of the source term, for which x^* is located at around 93% of the total domain length (see also Figure 5.5). This numerical result is similar to the one obtained in [29] in the case of a 1D Laplace equation coupled to a 2D Laplace equation.

CPU time. Finally, in Table 5.1, we compare the CPU time needed to compute the global reference solution on the whole domain (477 seconds in our case) with the CPU time needed to solve the Schwarz coupling algorithm. According to the convergence results in Figure 5.7, we choose to measure the CPU time after 5 and 10 iterations, since it corresponds to a rather good convergence and a small modeling

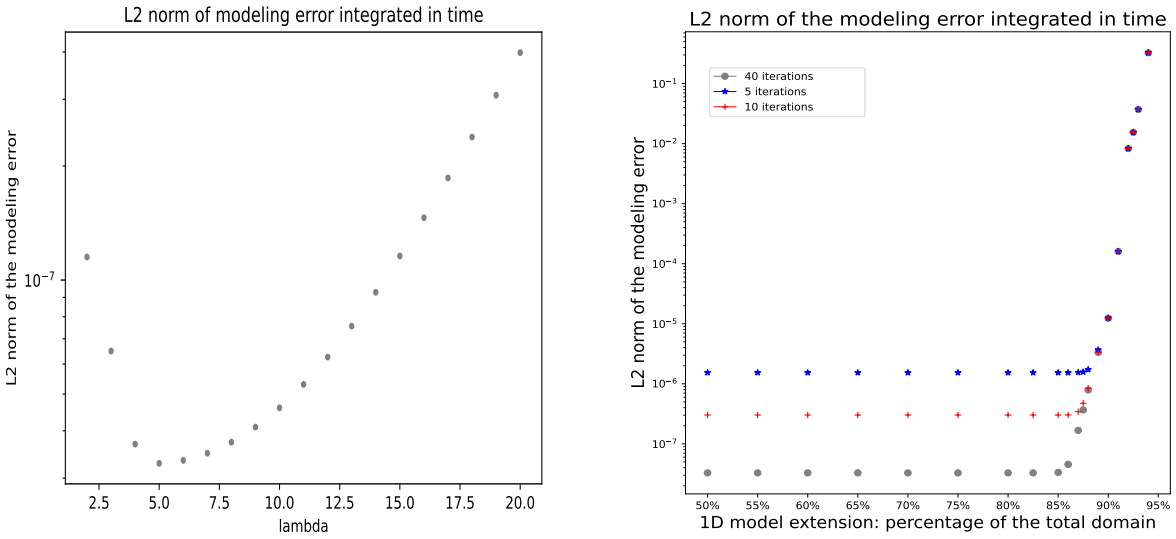

(A) (B)

FIGURE 5.8. Left panel: Time integrated L^2 norm of the modeling error, as a function of λ. Right panel: Time integrated L^2 norm of the modeling error after 5, 10 and 40 iterations, as a function of the interface position (expressed as a percentage of the total length of the domain).

error, as shown in Figure 5.8 (b), if the interface position remains in the zone where the vertical effects are small enough. We added also two time measurements after 40 iterations.

One of the main objectives of the coupling algorithm is, of course, to minimise CPU time without compromising the precision too much. In this context, when we consider 10 iterations, the CPU time is smaller than for the reference simulation when the interface position is optimal. In the case of 5 iterations, the CPU time is smaller for almost all tested interface positions (even far from optimal). As expected, if the total number of iteration is large (40 here), and without overlapping, the coupling algorithm loses its advantage compared to a direct execution of the NS system throughout the whole domain.

TABLE 5.1. CPU time (in seconds) as a function of the extension of the 1D model and of the amount of iterations. The values correspond to the average obtained from three executions of the code. The time needed to compute the global reference solution on the whole domain is 477 seconds.

Total number of iterations \ Interface position	**50**%	**60**%	**70**%	**80**%	**85**%
5	581	465	357	248	197
10	1120	910	700	484	379
40	-	-	-	2032	1703

6. Conclusion

We presented in this work a theoretical analysis of a Schwarz-like algorithm to couple the 3D linearized hydrostatic Navier–Stokes system with corresponding 2D linearized shallow water system obtained from the 3D equations under a small aspect ratio hypothesis. After introducing the iterative coupling

method, we prove that, if we assume a frictionless condition at the bottom, the convergence of the coupling algorithm is equivalent to the convergence of classical domain decomposition method applied to the shallow water system. The other main contribution of this work is the control of the modeling error as a function of the coupling interface location. This work can be extended in several directions: numerical optimization of the convergence rate of the domain decomposition algorithm for the linearized shallow water equation, numerical implementation and theoretical study of an overlapping coupling algorithm, study of the sensitivity of the modeling error to the aspect ratio, or set-up of a method to calculate the optimal interface location. Moreover, if we consider a non-zero friction on the bottom, which is often the case in real applications, there is no more equivalence between the convergence of the coupling algorithm and the convergence of the classical domain decomposition of the shallow water system. Therefore the convergence of the multi-dimensional coupling algorithm with Robin-type conditions, as well as the control of the modeling error, could be more complicated to obtain. This is essentially due to the expression of the extension operator: the quantities coming from the 2D model are no more uniformly extended on the vertical through the interface, but rather follow a parabolic distribution. The study of this case is therefore an interesting alternative. This work is also a first step for more realistic coupling problems of 2D shallow water system and 3D hydrostatic or nonhydrostatic Navier–Stokes systems, and for coupled problems involving other related systems like for instance moment shallow water models [16]. The most challenging perspective of the present work remains the design of a Schwarz algorithm to couple dimensionally heterogeneous nonlinear systems.

Acknowledgements

This work was partially supported by the research department of the French national electricity company, EDF R&D.

References

[1] C. Acary-Robert, E. Blayo, and M. Tayachi Pigeonnat. Schwarz algorithm implementation, 2025. `https://hal.science/hal-05253992v3`.

[2] A. Arakawa and V. Lamb. Computational Design of the Basic Dynamical Processes of the UCLA General Circulation Model. *Methods Comp. Phys.*, 17:173–265, 1977.

[3] E. Audusse, P. Dreyfuss, and B. Merlet. Schwarz waveform relaxation for primitive equations of the ocean. *SIAM J. Sci. Comput.*, 32(5):2908–2936, 2010.

[4] P. Blanco, M. Discacciati, and A. Quarteroni. Modeling dimensionally-heterogeneous problems: analysis, approximation and applications. *Numer. Math.*, 119(2):299–335, 2011.

[5] E. Blayo and L. Debreu. Revisiting open boundary conditions from the point of view of characteristic variables. *Ocean Model.*, 9:231–252, 2005.

[6] E. Blayo, A. Rousseau, and M. Tayachi. Boundary conditions and Schwarz waveform relaxation method for linear viscous shallow water equations in hydrodynamics. *SMAI J. Comput. Math.*, 3:117–137, 2017.

[7] M. P. Daou, E. Blayo, A. Rousseau, O. Bertrand, M. Tayachi Pigeonnat, C. Coulet, and N. Goutal. Coupling 3D Navier–Stokes and 1D shallow water models. In *Simhydro 2014*, 2014.

[8] A. Decoene. *Modèle hydrostatique pour les écoulements à surface libre tridimensionnels et schémas numériques*. PhD thesis, Université Paris 6, 2006.

[9] P. Finaud-Guyot, C. Delenne, V. Guinot, and L. Cecile. 1D–2D coupling for river flow modeling. *Comptes Rendus. Mécanique*, 339:226–234, 2011.

[10] L. Formaggia, J.-F. Gerbeau, F. Nobile, and A. Quarteroni. On the coupling of 3D and 1D Navier-Stokes equations for flow problems in compliant vessels. *Comput. Methods Appl. Mech. Eng.*, 191:561–582, 2001.

[11] M. Gander. Optimized Schwarz methods. *SIAM J. Numer. Anal.*, 44(2):699–731, 2006.

[12] M. Gander. Schwarz methods over the course of time. *Electron. Trans. Numer. Anal.*, 31:228–255, 2008.

[13] M. Gander, L. Halpern, and F. Nataf. Optimal convergence for overlapping and non-overlapping Schwarz waveform relaxation. In *Eleventh International Conference on Domain Decomposition Methods*, pages 27–36, 1999. `http://www.ddm.org/DD11/Gander.pdf`.

[14] J.-F. Gerbeau and B. Perthame. Derivation of viscous Saint-Venant system for laminar shallow water; numerical validation. *Discrete Contin. Dyn. Syst.*, 1(1):89–102, 2001.

[15] J. Koellermeier and H. Vandecasteele. Hierarchical micro-macro acceleration for moment models of kinetic equations. *J. Comput. Phys.*, 488: article no. 112194 (24 pages), 2023.

[16] J. Kowalski and M. Torrilhon. Moment Approximations and Model Cascades for Shallow Flow. *Commun. Comput. Phys.*, 25(3):669–702, 2019.

[17] J. Leiva, P. Blanco, and G. Buscaglia. Partitioned analysis for dimensionally-heterogeneous hydraulic networks. *Multiscale Model. Simul.*, 9:872–903, 2011.

[18] J.-L. Lions, R. Temam, and S. Wang. On the equations of the large-scale ocean. *Nonlinearity*, 5(5):1007–1053, 1992.

[19] N. Malleron, F. Zaoui, N. Goutal, and T. Morel. On the use of a high-performance framework for efficient model coupling in hydroinformatics. *Environ. Modell. Software*, 26:1747–1758, 2011.

[20] J. Marin and J. Monnier. Superposition of local zoom models and simultaneous calibration for 1D–2D shallow water flows. *Math. Comput. Simul.*, 80:547–560, 2009.

[21] V. Martin. Schwarz waveform relaxation algorithms for the linear viscous equatorial shallow water equations. *SIAM J. Sci. Comput.*, 31:3595–3625, 2009.

[22] E. Miglio, S. Perotto, and F. Saleri. Model coupling techniques for free-surface flow problems: Part I. *Nonlinear Anal., Theory Methods Appl.*, 63:e1885–e1896, 2005.

[23] F. Mintgen and M. Manhart. A bi-directional coupling of 2D shallow water and 3D Reynolds-averaged Navier–Stokes models. *J. Hydraul. Res.*, 56(6):771–785, 2018.

[24] G. Panasenko. Method of asymptotic partial decomposition of domain. *Math. Models Methods Appl. Sci.*, 8(1):139–156, 1998.

[25] S. Pantazis and H. Rusche. A hybrid continuum-particle solver for unsteady rarefied gas flows. *Vacuum*, 109:275–283, 2014.

[26] A. Rousseau. *Etudes théoriques et numériques des équations primitives de l'océan sans viscosité*. PhD thesis, Université Paris XI Orsay, 2005.

[27] A. Rousseau, R. Temam, and J. Tribbia. Boundary value problems for the inviscid primitive equations in limited domain. In P. G. Ciarlet, R. Temam, and J. Tribbia, editors, *Computational Methods for the Atmosphere and the Oceans*, volume 14 of *Handbook of Numerical Analysis*, pages 481–576. Elsevier, 2008.

[28] M. Tayachi. *Couplage de modèles de dimensions hétérogènes et application en hydrodynamique*. PhD thesis, University of Grenoble, 2013.

[29] M. Tayachi Pigeonnat, A. Rousseau, E. Blayo, N. Goutal, and V. Martin. Design and analysis of a Schwarz coupling method for a dimensionally heterogeneous problem. *Int. J. Numer. Methods Fluids*, 75(6):446–465, 2014.